Toward Intelligent Molecular Machines: Directed Motions of Biological and Artificial Molecules and Assemblies

Kazushi Kinbara[†,‡] and Takuzo Aida*,[†]

Department of Chemistry and Biotechnology, School of Engineering, The University of Tokyo, 7-3-1 Hongo, Bunkyo-ku, Tokyo 113-8656, Japan, and PRESTO, Japan Science and Technology Agency (JST), 4-1-8 Honcho, Kawaguchi, Saitama 332-0012, Japan

Contents

[†] The University of Tokyo.
[‡] PRESTO.

1. Introduction

In the last two decades, considerable progress has been made in the field of molecular biology, which has enabled a molecular-level understanding of a number of interesting biological events. In particular, the discovery of a family of moving proteins and their assemblies has attracted particular attention not only of biologists but also of chemists and physicists.[1−5] In response to certain biological stimuli, these proteins perform directed or programmed motions, similar to many tools and machines used in our daily life. Such biological molecular machines play essential roles in a wide variety of biological events, particularly those related to the activities of cells,[1] and realize specific functions through their stimuli-responsive mechanical motions.

Cytoplasmic proteins such as myosins, kinesins, and dyneins are called "molecular motors" and are the most extensively studied molecular machines.[2−5] These protein-based supramolecular conjugates are known to switch back and forth along linear tracks of actin filaments or microtubules and transport substrates at the expense of adenosine triphosphate (ATP) as fuel. The flagellum is a huge protein conjugate that controls the swimming motion of bacteria.[6] The bacterial flagellar motor consists of (1) flagellar filaments that are 15 μm long and 120−250 Å in diameter and a (2) motor domain that rotates the flagellar filaments alternately in clockwise and anticlockwise directions. This unique behavior of rotation allows bacteria to swim desirably. ATP synthase is a different type of a molecular machine, which synthesizes and hydrolyzes ATP through its rotary motion.[7−9] ATP synthase is built up of two different machinery components, that is, F_1 and F_0, where the rotation of the former is driven by the free energy released from the hydrolysis of ATP to adenosine diphosphate (ADP); the latter rotates by a flux of ions passing through a membrane and synthesizes ATP. This huge protein complex has a shaft, which rotates just like real rotary motors. Since the rotary motion of ATP synthase occurs in a stepwise manner in response to the hydrolysis of ATP, it is regarded as a biological stepping motor. In addition to these molecular motors, some other biological machines are known, where the hydrolysis of ATP triggers different types of mechanical motions. Representative examples include the family of chap-

Dr. Kazushi Kinbara was born in 1967. He received a B.S. degree in Organic Chemistry from the University of Tokyo in 1991 and obtained a Ph.D. in Organic Chemistry in 1996 under the direction of Professor Kazuhiko Saigo. He then began an academic career at The University of Tokyo and had been involved until 1999 in the development of optical resolution upon crystallization. In 1999, he moved to the Department of Integrated Biosciences, Graduate School of Frontier Sciences, The University of Tokyo. In 2001, he was promoted to Lecturer of the Department of Chemistry and Biotechnology, School of Engineering, The University of Tokyo. In 2003, he was selected as a researcher of the JST PRESTO project "Light and Control". His research interests include (1) artificial and biological molecular machineries, (2) organic syntheses under the control of supramolecular systems, and (3) crystal engineering.

Dr. Takuzo Aida was born in 1956. He received a B.S. degree in Physical Chemistry from Yokohama National University in 1979 and then studied at The University of Tokyo, obtaining a Ph.D. in Polymer Chemistry in 1984. He then began an academic career at The University of Tokyo and had been involved until 1994 in the development of precision macromolecular synthesis using metalloporphyrin complexes. In 1996, he was promoted to Full Professor of the Department of Chemistry and Biotechnology, School of Engineering, The University of Tokyo. His research interests include (1) controlled macromolecular synthesis with mesoporous inorganic materials, (2) photo- and supramolecular chemistry of dendritic macromolecules, (3) mesoscopic materials sciences, and (4) bio-related molecular recognitions and catalyses. In 1996, he was appointed as a researcher of the JST PRESTO project "Fields and Reactions". In 2000, he was then selected as the leader of the ERATO project on "NANOSPACE".

eronin proteins, which adopt cylindrical shapes and are capable of entrapping guest molecules, such as denatured proteins, to assist in their refolding.[10] The hydrolysis of ATP results in an open−close conformational motion of the cylindrical cavity, thereby triggering the release of guest molecules. Such biological molecular machines also include helicases[11] and ribosomes,[12] which move along the strands of nucleic acids. These biological molecular machines consist of different movable parts that are interlocked

to achieve directed motions. Thus, these machines are potential components in the fabrication of intelligent nanodevices. Semibiological molecular machines with DNA-based components have also been reported, where stimuli-responsive transitions of DNA strands are utilized to realize machine-like directed motions.[13] Along with these biological and semibiological approaches, the design of artificial or fully synthetic molecular machines, capable of performing directed motions similar to those of biological machines, has attracted long-term attention.[14−17]

The present article gives an overview of the studies on biological molecular machines, with an emphasis on their "programmed" motions and potential applications to the fabrication of movable nanodevices. The article also includes selected examples of semibiological and fully synthetic molecules and related assemblies that are capable of performing directed motions in response to certain stimuli. One of the aims of this review is to bring together the research areas of biological and artificial molecular machineries, which have most often been discussed separately, and to initiate a new paradigm for the development of intelligent nanodevices.

2. Biological Molecular Machines

2.1. Myosins

Myosins are molecular motors that move along actin filaments and have attracted attention for more than a century. Myosins bind to actin filaments (F-actin) to form actomyosins and walk unidirectionally along the filament.[1] An actin filament is a double-helical supramolecular polymer of actin monomers (g-actin: globular actin) with a pitch of 36 nm (Figure 1).[18,19] One pitch includes 13 actin monomers. Myosins comprise a superfamily consisting of 18 different classes with a variety of properties tailored for cellular activities such as muscle contraction, vesicle transport, membrane trafficking, cell locomotion, cytoplasmic streaming, and signal transduction.[20−23]

2.1.1. Structural Aspects of Myosins

Myosins consist of one or two "heavy chains", with a molecular mass of ca. 200 kDa, and one to six "light chains", with a molecular mass of ca. 20 kDa, that wrap around the neck region of the heavy chain just like a necklace (Figure 2). The structure of the myosin heavy chain can be divided into three domains according to their roles. The first domain, located at the *N*-terminal of the heavy chain, has an actin-binding site and serves as the motor. On the opposite side of the actin-binding site is an ATP-binding site where the hydrolysis of ATP occurs. The second domain includes a tail, which assembles and positions the motor domains properly so that they can interact with the actin filament. In some cases, the tail domain is bound to cargo. Certain myosins are known to contain within the tail domain a coiled-coil-forming region, which allows the dimerization of the heavy chain. Such myosins are called double-headed myosins. The last domain forms a neck that is connected to the light chains and calmodulin and
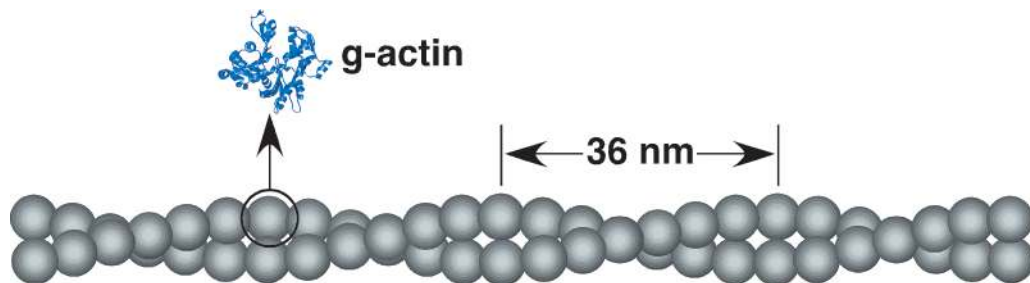
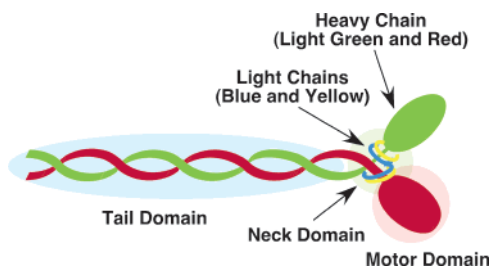**Figure 1.** Schematic representation of an actin filament (f-actin).

Figure 2. Schematic structure of double-headed myosin composed of heavy and light chains.

serves as the "lever arm", where a power stroke is generated through the hydrolysis of ATP. Upon treatment with a protease (trypsin), myosins are cleaved into two stable fragments, one of which, including the motor domain, is called heavy-mero-myosin (HMM), while the other, carrying the tail domain, is called light-meromyosin (LMM).[24] The motor domain of HMM preserves the ATPase activity of the parent myosin and can walk along an actin filament. Therefore, HMM has been investigated as the smallest component of myosins. The following sections highlight myosin II and myosin V, which have been the most intensively studied myosins toward a mechanistic understanding of the biological motions of the myosin superfamily.

2.1.2. Chemomechanical Properties and Application of Myosin II

Myosin II is responsible for muscle contraction. It was isolated in 1864[25] and is frequently called the "conventional myosin". The motion of myosin II has become better understood since 1993, when the crystal structure of a subfragment including the motor domain was solved by Rayment and co-workers (Figure 3).[26,27]

Myosin II is a dimeric protein with two motor domains that moves along the actin filament from the minus to the plus ends. In the actual muscle system, myosin II forms thick filaments, which assemble with actin filaments to form a "sarcomere". For the motion of myosin II, the "swinging lever-arm" mechanism is currently a widely accepted model (Figure 4).[28] This model includes a catalytic ATPase cycle consisting of four fundamental steps. In the initial stage, myosin II is strongly bound to an actin filament to form actomyosin (AM). In the second step, binding of ATP takes place at an empty site located at the motor domain of actomyosin, lowering the affinity of the motor domain toward the actin fila-ment. Consequently, actomyosin is dissociated into the ATP−myosin II conjugate and the actin filament.

Figure 3. Crystal structure of myosin II subfragment S1. The blue segment represents a heavy chain, while green and red segments represent light chains.
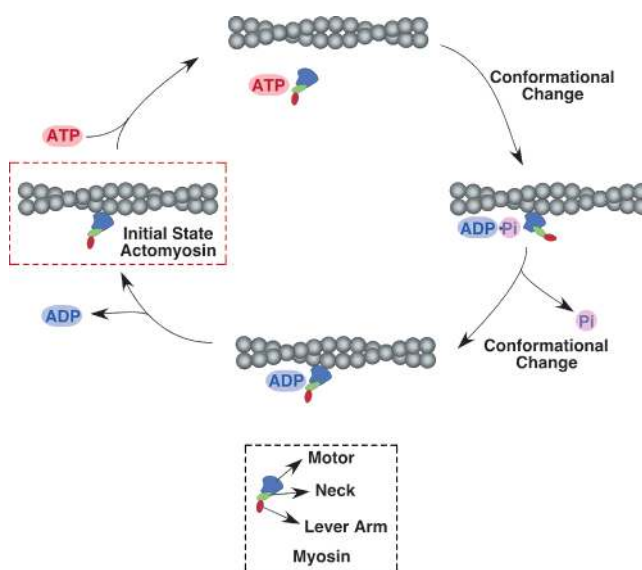
Figure 4. Schematic representation of the ATPase cycle involving myosin II and actin filament. The cycle consists of four fundamental steps initiated by the addition of ATP to actomyosin.

The binding of ATP also triggers a conformational change of the neck domain to give rise to a pivotal motion on the motor domain. The third step involves hydrolysis of the ATP−myosin II conjugate to give a complex of an ADP−myosin II conjugate and phos-phate Pi (ADP·Pi−myosin II), which is then bound to the actin filament. Since ADP·Pi−myosin II has a lower affinity than myosin II toward the actin fila-ment, the composite of ADP·Pi−myosin II with the
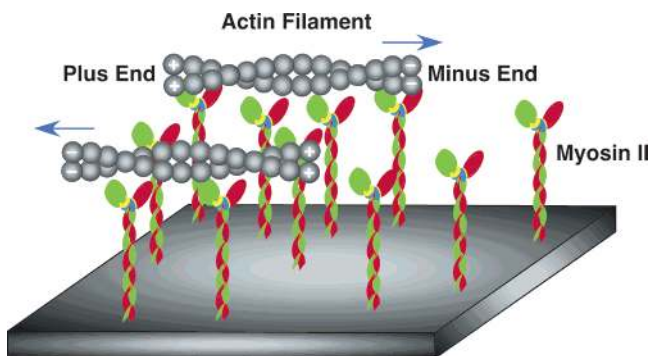
Figure 5. Directed motion of actin filaments from plus to minus ends on an immobilized myosin surface. On addition of ATP, a fluorescently labeled actin filament moves on a glass surface coated with myosin II.

Figure 6. Schematic structure of double-headed myosin V composed of cargo-binding, tail, neck, and motor domains. Red and green segments represent heavy chains, while blue and yellow segments represent light chains.

actin filament is called a "weak binding state". In the final step, the ADP·Pi–myosin II/actin filament conjugate releases ADP and Pi stepwise. This results in a conformational change of the motor domain, so that the neck domain is tilted by almost 90° toward the axis of the actin filament. This motion leads to the contraction of muscles and is called the "power stroke". When ADP is released, the cycle returns to the initial stage, that is, ATP-free actomyosin. This model is supported by X-ray crystallographic studies and many analyses.[29–35]

Recently, a different mechanism involving the "biased Brownian ratchet model"[36] has been reported by Yanagida and co-workers.[37,38] In this model, the sliding motion of myosin II on the actin filament is driven by a directionally biased Brownian motion. Some experimental results have suggested that the hydrolysis of one molecule of ATP allows myosin II to move a longer distance than expected from the previous model.[39–41] By means of single-molecule imaging combined with a laser trapping technique, Yanagida et al. have shown that myosin II moves in both the forward and backward directions in 9:1 ratio with regular steps of 5.3 nm.[40,42]

Myosin II also moves in "in vitro" systems and may be integrated into nanomechanical devices.[43,44] Kron and Spudich have reported that a fluorescently labeled actin filament can move by the action of ATP on a glass surface coated with myosin II (Figure 5).[45] This system can be regarded as a "nanoactuator", and many related examples have been reported thereafter.[46] For example, Suzuki and Nicolau have succeeded in detecting the directional motion of actin filaments on myosin molecules aligned and immobilized on a shallow track that was microlithographically drawn on a polymer surface.[47] More recently, Månsson, Bunk, and co-workers have shown that the actin filament moves only unidirectionally without U-turns in a much narrower track, drawn by an electron-beam technique.[48,49] External forces may be useful for controlling the motion of myosin II. For example, Matsunaga and co-workers have prepared myosin II attached to a magnetic particle separated from magnetic bacterium and have tried to control its movement on actin filaments with a magnetic force.[50]
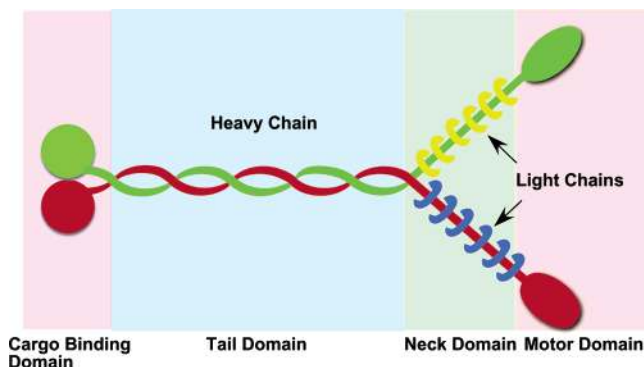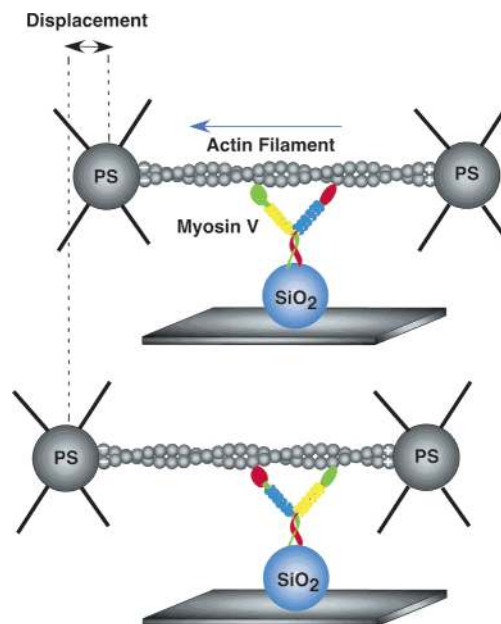
Figure 7. Optical trapping assay of directed motion of actin filament on myosin V immobilized on a silica bead. An actin filament is attached to polystyrene beads at both ends and allowed to interact with myosin V, immobilized on a silica bead.

2.1.3. Chemomechanical Properties and Application of Myosin V

Myosin V transports a variety of intracellular cargo, including organelles, along actin filaments.[1,51] Myosin V is a dimeric myosin having two motor domains (Figure 6). In 1999, Metha, Cheney, and co-workers reported that the motion of mammalian myosin V is processive.[52] The term "processivity" means a nondissociate walking motion along an actin filament. This pioneering study has contributed significantly to the mechanistic understanding of the motility of myosin V.

For continuous monitoring of the motion of actin filaments, the group of Metha and Cheney has developed an optical trapping assay system, where an actin filament, attached to polystyrene beads at both ends, is allowed to interact with myosin V, immobilized on a silica bead (Figure 7).[52] In a study with this monitoring system, they have shown that myosin V moves processively in large steps ap-

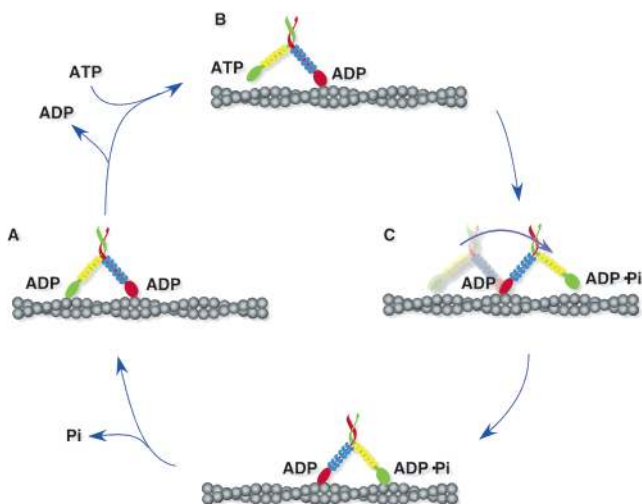**Figure 8.** Schematic representation of the ATPase cycle of myosin V moving along an actin filament. In the two-head-bound state (A), the leading and trailing heads, both conjugated with ADP, are attached to the actin filament. The cycle is initiated by the replacement of one of the two ADP molecules with ATP.

Figure 9. Schematic representations of the hierarchical structure of microtubules. Microtubules are assemblies of protofilaments, which are formed by the head-to-tail self-assembly of a heterodimer of two different protein subunits called α- and β-tubulins (orange and purple segments, respectively).

proximating the 36-nm helical pitch of the actin filament at every hydrolysis event of an ATP molecule. The processive motion of myosin V has also been supported by an observation that myosin V (fluorescently labeled) continuously moves over a long distance (several microns) unidirectionally.[53] If the dissociation/reassociation occurs frequently, myosin V could stop in a shorter walking distance or go back and forth between short distances. For this movement, the "hand-over-hand" mechanism has been proposed.[54,55] Figure 8 schematically shows a currently accepted mechanism for the processive movement of myosin V along the actin filament.[56] The first step involves a two-head-bound state, where the leading and trailing heads, conjugated with ADP, are both attached to the actin filament (Figure 8A). A possible unbalanced tension between the two attached heads promotes the selective release of ADP from the trailing head. After the release of ADP, ATP is bound to the resulting vacant site and triggers the dissociation of the trailing head from the actin filament (Figure 8B). At this stage, the leading head swings its neck domain (lever arm) to throw the trailing head in front. The new leading head, thus formed, hydrolyzes ATP to become an ADP·Pi conjugate, which then rebounds preferentially to an actin subunit in front of the partner head (Figure 8C). Subsequently, the resultant actin-bound ADP·Pi conjugate releases phosphate Pi and returns to the initial two-head-bound state (Figure 8A). In this way, the myosin V dimer moves in a "hand-over-hand" manner along the actin filament. Current mechanistic studies on the motility of myosin V have focused on its structural dynamics at the individual steps.[57]

The processive motion of myosin V has the potential for the fabrication of artificial cargo-carrying systems similar to those with kinesins described in the following section. However, such applications require tricks to align actomyosin. Superfine and co-workers have reported two-dimensional manipulation and orientation of actin filaments by means of di-
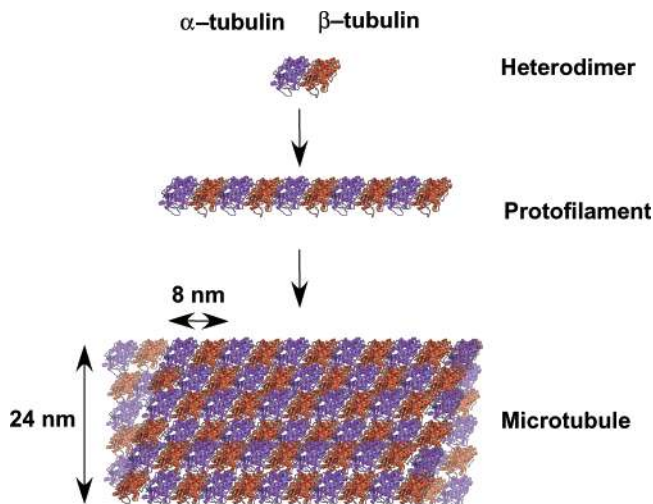
electrophoresis,[58] where actin filaments can be aligned along electric field gradients using quadruple electrodes fabricated on a glass surface.

2.2. Kinesins

Kinesins are molecular motors that move along microtubules and were discovered in 1985.[59] They are involved in the intracellular transport of organelles, protein complexes, and mRNAs, and they also participate in chromosomal and spindle movements during mitosis and meiosis. While myosins move along actin filaments, kinesins walk along microtubules, which are hollow tubular assemblies having a diameter of 24 nm and an 8-nm structural periodicity, and are larger than the actin filaments. Microtubules are assemblies of protofilaments, which are formed by the head-to-tail self-assembly of a heterodimer of two different protein subunits called α- and β-tubulins (Figure 9).[1,60,61] Microtubules have a polarity with fast-growing (plus) and slow-growing (minus) ends, and kinesins are allowed to move unidirectionally using their motor domain on the microtubules.[62] Kinesins compose a superfamily (KIFs). While the superfamily is categorized into 14 taxonomic groups,[63] it is classified into three major types. that is, *N*-terminal (11 classes), middle motor domain (2 classes), and *C*-terminal kinesins (1 class), depending on the topology of the motor domain.

2.2.1. Structural Aspects of Kinesins

Conventional kinesin and kinesin heavy chain (KHC) both belong to the N-1 class and have been studied most extensively. Conventional kinesin is ubiquitous and expressed in many tissues,[64] and it consists of two 80-nm long heavy chains (120 kDa), which are connected at their *C*-termini to two light chains (64 kDa). Each heavy chain has a rodlike structure composed of two globular heads, a stalk, and fanlike ends (Figure 10)[1,65,66] and carries at the *N*-terminus a motor domain bearing ATP- and mi-
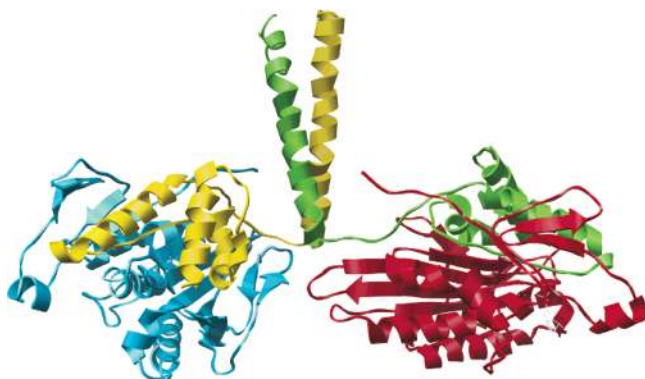
Figure 10. Crystal structure of the kinesin dimer from *Rattus Norvegicus*. Blue/red subunits and yellow/green subunits are structurally identical pairs.

crotubule-binding sites. The motor domain has a structural homology with those of myosins.[67] The N-1 class also includes two highly related members, which are expressed in the nervous system.[68] Although most kinesins are two-headed, one-headed kinesin, consisting of single heavy and light chains, also exists[69] and has been reported to move processively along a microtubule, similar to two-headed conventional kinesin.[70,71]

2.2.2. Chemomechanical Properties of Kinesin Motors

Early studies on the mechanism of ATP hydrolysis and related motions of kinesins have been carried out with genetically engineered one-headed kinesins,[72,73] and the following model has been proposed.[1] In the first step, ADP is tightly bound to the kinesin head, and the resultant conjugate is connected to a microtubule. Then, ADP is released, thereby allowing the motor domain to be bound to the microtubule more tightly. In the second step, ATP is bound to the kinesin/microtubule conjugate. This event can occur rapidly and enhance the stability of the conjugate. Then, a structural change, leading to the movement of kinesin, immediately takes place.

Later, the motion of two-headed kinesins was investigated by combining biochemical and structural data for the ATP-hydrolysis cycle established with one-headed kinesins. Figure 11 shows the currently accepted mechanism involving a chemomechanical model for conventional kinesin, originally proposed by Hancock, Shief, and Howard, where the two motor domains attach to and detach from a microtubule alternately.[73,74] Thus, conventional kinesin moves along the microtubule from its minus to plus ends. Studies with a fluorescently labeled two-headed kinesin and laser trapping technique have suggested that conventional kinesin moves processively, making a discrete 8-nm step whenever it hydrolyzes exactly one ATP molecule.[75–77] Conventional kinesin, upon binding with ADP, immediately binds to a microtubule (Figure 11A). Then, ADP is released from either of the two heads to give a transition state, where one empty head is bound tightly to the microtubule in such a conformation that it may prevent the second head, conjugated with ADP, from binding to the microtubule (Figure 11B). Along with some biochemical data, cryo-electron microscopy (cryo-EM) has
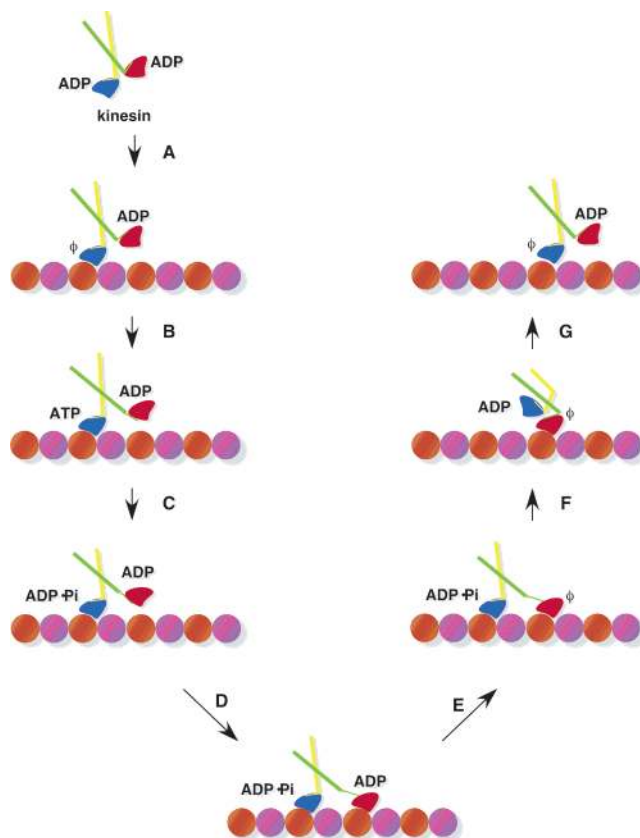

Figure 11. Schematic representation of the ATPase cycle involving kinesin and microtubule, where two motor domains attach to and detach from a microtubule alternately. Orange and purple circles represent α- and β-tubulins, respectively. The symbol ϕ indicates that the nucleotide-binding site is empty.

shown directly that, in the absence of nucleotides, one head of kinesin is bound to a microtubule, while the other remains free. In the next step, ATP is bound rapidly to the resulting guest-free motor domain attached to the microtubule, and then it is hydrolyzed to give a kinesin·Pi·ADP/microtubule conjugate (Figure 11C). Subsequently, binding of the residual head to the microtubule (Figure 11D), followed by a rapid release of ADP, takes place, thereby locking the motor domain into a two-head bound conformation (Figure 11E). This transition allows the two heads of kinesin to span 8 nm between successive tubulin subunits. To complete the hydrolysis cycle, the trailing head is detached after the release of Pi (Figure 11F) and swings toward the plus end of the microtubule (Figure 11G). Upon repetition of this cycle, conventional kinesin walks along a microtubule unidirectionally.

On the walking motion of two-headed kinesins, the "hand-over-hand" and "inchworm" mechanisms have been proposed.[78–81] However, Block and co-workers have reported that a certain kinesin moves with limping along the microtubule and proposed the "asymmetric hand-over-hand" walking model.[80] The main issue in these arguments stems from a consideration that the walking motion, which is asymmetric, should require the ATP hydrolysis to occur not simultaneously, but sequentially at the two head parts of kinesin. However, the two heads are composed of identical proteins and may hardly generate

an asymmetric conformational change, leading to the walking motion.

2.2.3. Application of Kinesin Motors

If kinesin−microtubule conjugates could be formed outside the cell, one may realize "molecular shuttles" that are capable of transporting cargo. From this point of view, substantial investigations have been made on the construction of in vitro shuttling systems using kinesin motors.[82,83] There are two approaches for the evaluation of such motor systems.[84−86] The first approach makes use of a "gliding assay", where kinesin is fixed on a substrate and microtubules are placed on its surface and allowed to move. In this approach, one can use optical microscopy for observing the motion of microtubules, since they are large enough to visualize. Another approach is called a "bead assay", where kinesins are allowed to walk on microtubules immobilized on a substrate surface. In this case, kinesins have to be fluorescently labeled for the visualization of their walking motions. As described in the above section, kinesin walks along a microtubule from its minus to plus ends. If cargo is to be transported in a certain direction using the movement of kinesin on microtubules, the kinesin should be added to a surface that is coated with microtubules that are aligned in polarity. On the contrary, microtubules can also be used as cargo carriers when placed on a substrate functionalized with kinesins. However, in this case, one has to consider some tricks for the unidirectional movement of all the microtubules.

Vogel and co-workers have utilized a highly oriented polymer film functionalized with kinesin and succeeded in driving microtubules in straight lines along the orientation axis of the film.[87] More recently, Hess and co-workers have reported a unidirectional motion of microtubules in a kinesin-immobilized 2-μm channel with two undercuts (1-μm height and 200-nm depth), prepared by photolithography.[88] Uyeda and co-workers have fabricated unidirectional arrowhead patterns and immobilized kinesin inside the patterns.[89] When microtubules are placed in these channels, they eventually move unidirectionally, since the movement of microtubules in the opposite direction of the arrowheads is difficult. On the basis of this technique, they have also succeeded in the construction of microminiaturized circulators, in which microtubules rotate unidirectionally. Furthermore, when two pools are connected by an arrowheaded track, microtubules are actively transported from one pool to the other in the direction of the arrowheads.

Some attempts on uniform alignments of microtubules have also been reported. Böhm and co-workers have shown that the flow of fluid can be used to orient microtubules into the same polarity.[90] In this case, constant flow is necessary to achieve a unidirectional gliding motion of microtubules on a immobilized kinesin surface. Stewart and co-workers have utilized a surface-immobilized antibody, that is complementary to the minus end of a microtubule, for asymmetric capturing, and they tried to orient the plus ends of the trapped microtubules downstream of the flow.[91] As the other approach, Hancock et al. have utilized short seeds of immobilized microtubules on a substrate surface for initiating the polymerization of tubulins, and they successfully obtained an oriented microtubule array.[92]

Shuttling of cargo has also been reported. Limberis and co-workers have investigated the movement of a silicon microchip by kinesin on an immobilized microtubule under fluid flow conditions on a substrate surface.[93] As observed by differential interference contrast (DIC) light microscopy, some of the chips are translated, while others are rotated or flipped over. Böhm and co-workers have reported that cargo such as glass beads, gold particles, and polystyrene beads (diameter 1−10 μm) is unidirectionally translocated by kinesin on microtubules aligned parallel in an isopolar fashion in a much stronger fluid flow.[94] A more recent example includes the transport of CdSe nanoparticles.[95]

The groups of Hess and Vogel have developed several different kinesin-based nanodevices.[82,83] For example, the strengths of weak intermolecular bonds have been measured by a kinesin−microtubule conjugate,[96] and the system is called a "piconewton forcemeter". When a streptavidin−biotin complex is submitted to this kinesin-based forcemeter, it dissociates at an applied force larger than 5 pN. They have also shown that shuttling motion can be controlled by light.[97] Kinesin moves along a microtubule at the expense of ATP. When "caged ATP"[98] is used as a fuel, ATP is released upon irradiation with ultraviolet light and drives the motion of kinesin. By using this trick, one can reversibly turn on and off the transportation of cargo in response to ultraviolet light.

2.3. Dyneins

Dyneins are protein conjugates located in eukaryotic cells. Dyneins placed on microtubules carry cargo toward the minus end of the track.[99−101] Dyneins are involved in diverse fundamental cellular processes including mitosis, vesicular transport, and the assembly and motility of cilia and flagella. Nearly 15 forms of dynein have been found in vertebrates, which are mostly "axonemal", meaning that they are associated with ciliary and flagellar movements, while only two forms are "cytoplasmic".[1,101] Dyneins also consume ATP as a fuel for the machinery.

In general, dyneins have very high molecular weights, and their structures have not been well established. Dyneins include heavy chains (∼520 kDa), which possess a motor domain with six ATPase units. The molecular weight of the motor domain is 10 times as large as that of conventional kinesin. Dyneins also contain a variety of additional subunits called intermediate chains (ICs), light intermediate chains (LICs), and light chains (LCs). Some of these components are common to cytoplasmic and axonemal dyneins, whereas others are specific to dynein subclasses. Dyneins are members of the ancient AAA+ family of ATPases.[102,103] As a common structural feature, the AAA+ family members possess a hexameric ring consisting of ca. 35 kDa AAA ATPase domains (Figure 12). In dyneins, the six ATPase units are integrated in a single polypeptide chain to form
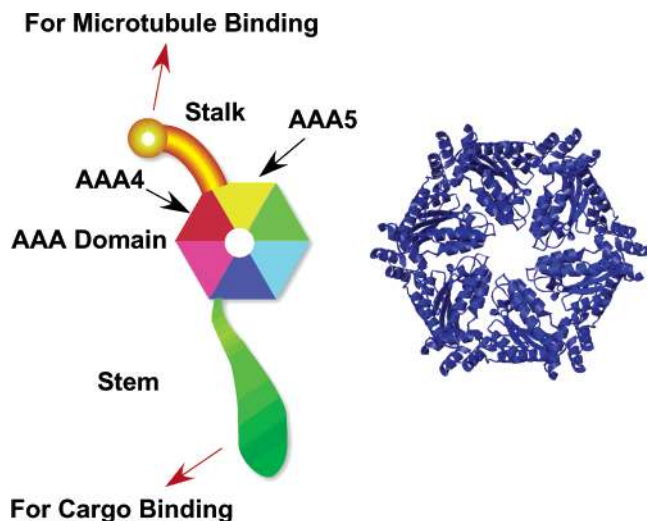
Figure 12. Schematic structure of dynein (left) and crystal structure of the ATPase domain (right) of AAA protein NSF.

Figure 13. Schematic structure of the bacterial flagellar motor, composed of several fundamental parts such as filament, hook, bushing, rod, stator, and rotor, each consisting of one or more protein subunits.

a ring. This structural feature is conserved in all dyneins, from axonemal to cytoplasmic ones, at their heavy chains. Dyneins possess two additional domains, projected out of the hexameric ring, which play an essential role in the function. One of these domains is called a "stalk", which is 15-nm long and emerges between AAA4 and AAA5. The stalk carries an ATP-sensitive microtubule-binding site at its tip. The *N*-terminal region of the hexameric ring is connected to the other projecting object, which is larger and referred to as the "stem", capable of docking with a cargo.

Recently, Burgess, Knight, and co-workers have reported an electron micrograph of a dynein, which is informative of the in vitro motion of this huge protein conjugate.[104,105] In a cycle of ATP hydrolysis, release of ADP and phosphate from dynein results in the power stroke motion. On hydrolysis of ATP to ADP, a part of the stem closest to the AAA ring likely folds up and lies against one face of the ring. A change in the interaction between the stem and the hexameric ring has been suggested to play a crucial role in force generation. The structural visualization of the motor domain is awaited for better understanding of the mechanism of the power stroke.

2.4. Bacterial Flagella

Many species of bacteria such as *E. coli* swim using rotary motors attached to helical filaments called flagella.[1,106] The highly organized motor exists at the cell envelope and is driven by a flux of ions across the cytoplasmic membrane. Thus, flagellar motors are different from linear motors of eukaryotes, which are powered by the hydrolysis of ATP. A flagellar motor can rotate its filaments in both clockwise and counterclockwise directions.

The bacterial flagellar motor is one of the most complicated objects found in bacteria and contains more than 40 different proteins. It is 45 nm in diameter, having a $10-15$ μm long filament, and consists of numerous protein subunits. Figure 13 shows a schematic structure of the bacterial flagellar motor, which is composed of several fundamental
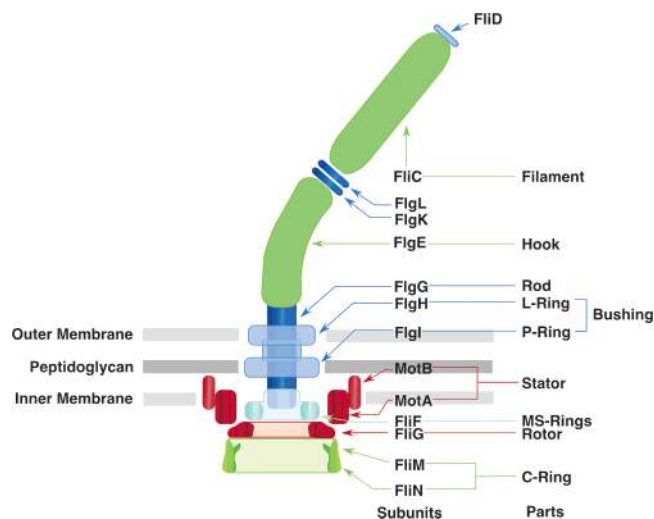
parts such as filament, hook, bushing, rod, stator, and rotor, each consisting of one or more protein subunits. The filament and hook jointly work as a propeller for driving cells. The motor is composed of a rotor and a stator, and the flagellum is connected to the motor through a rod embedded in a bushing. The essential part of the machinery is called the "basal-body", which involves L-, P-, and C-rings along with the above-mentioned stator, rotor, and rod. The torque-generating part of the machine involves five proteins: MotA, MotB, FliG, FliM, and FliN.[107] The latter three proteins are referred to as the "switch complexes", as the switching function of the rotational direction is disabled upon mutation of these proteins.[108,109] The C-ring, composed of $34-35$ molecules of assembled FliM and FliN,[110,111] is capped by a conjugate of the M- and S-rings called the MS-ring, which consists of 26 molecules of FliF.[112] The MS-ring is bound to the C-ring via a ring-shaped assembly of FliG located on the cytoplasmic surface. The rotor (FliG) transfers its torque to the MS-ring and then to the filament. The stator is composed of MotA and MotB, which are embedded in a membrane. Studies with electron microscopy have revealed that eight MotA and MotB molecules are assembled together to surround the rotor to form the "studs".[113] The MotA−MotB conjugate serves as a proton channel and generates a torque. Mutation studies[114] on MotA and MotB have shown that the torque is generated through protonation and deprotonation at Asp32 in MotB. Consequently, a conformational motion takes place in MotA and triggers the rotary motion of the rotor part (FliG) by changing the electrostatic interaction of the cytoplasmic domain of MotA with the C-terminal domain of FliG (Figure 14).[115] The mismatch in the numbers of protein molecules between the C-ring ($34-35$) and the MS-ring (26) has also been considered responsible for the torque generation. Recently, a part of FliG has been crystallographically defined by Lloyd and co-workers.[116] The structure is informative of the mechanism of the torque generation. The rod included in the basal body consists of five different
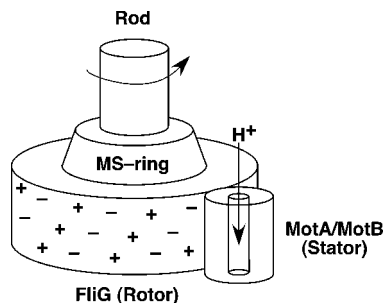
Figure 14. One of the proposed mechanisms for the rotary motion of the bacterial flagellar motor. Through protonation and deprotonation at Asp32 in MotB, a conformational motion takes place in MotA and triggers the rotary motion of the rotor part (FliG).

Figure 15. Schematic structure of ATP synthase composed of F_1 ($\alpha-\epsilon$) and F_0 (a–c). Both F_0 and F_1 act as motors, which are driven by protons and ATP, respectively.

proteins (FliE, FlgB, FlgC, FlgF, and FlgG), while the bushing part in the cellular membrane is composed of L- and P-rings and threaded by the rod. The hook and filament parts are polymers of hook protein (FlgE) and flagellin (FliC, 25–60 kDa), respectively, which further assemble with three other proteins (FlgK, FlgL, and FliD) to form the propeller. The rod connects the propeller to the motor in the cell exterior.

The filament is composed of more than 10 000 copies of flagellin. Namba and co-workers have shown by cryo-electron microscopy that the filament is composed of 11 protofilaments of FliC. The protofilament is denoted as either R or L depending on the twisting direction.[117] When the 11 protofilaments are all R or L, the resulting filament adopts a right- or left-handed helical form with a straight shape. When there is a mixture of R- and L-protofilaments, the filament can adopt several different helical waveforms. The left-handed normal waveform propels cells during a run.

Although the bacterial flagellar motor is more powerful than other molecular motors,[118] devices that utilize the bacterial flagellar motor have not been developed. This fact is due to the difficulty in isolating functioning motors outside of the cell, since the motor components span the cell membrane. Darnton and co-workers[119] have demonstrated that bacterial cells can adhere to much larger objects (such as 10-μm beads or larger pieces of poly(dimethylsiloxane)) and propel them. The transport of smaller cargo on single cells may also be possible. The strategy of utilizing the existing motor machinery within swimming cells for the transport of cargo could lead to new, hybrid biodevices.

2.5. ATP Synthases

ATP synthases are one of the most sophisticated molecular machines in biological systems. ATP synthases are ubiquitous in all kinds of mammalian cells and require a proton gradient for the synthesis of ATP. On the contrary, if ATP is supplied, ATP synthases generate an ion gradient. The structure of the most essential part of ATP synthases is conserved throughout the evolution, although there are some variations in the number of subunits. In the following section structural and mechanistic aspects of bacte-
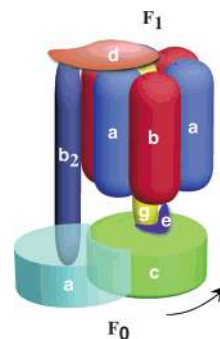
rial and mitochondrial ATP synthases are highlighted.

2.5.1. Structure of ATP Synthases

Bacterial and mitochondrial ATP synthases are large protein complexes consisting of two domains called F_0 and F_1 (Figure 15). Both F_0 and F_1 act as motors, which are driven by protons and ATP, respectively. The crystal structures of F_1 and a part of F_0 have been solved by Walker, Leslie, and co-workers[120,121] and are informative with regard to the conformational changes associated with the hydrolysis of ATP and the proton flux. F_1 represents the shaft part, which rotates relative to the surrounding portion (F_0). Due to their unique motions, F_0 and F_1 are called rotor and motor, respectively. Since F_0 and F_1 can reversibly be dissociated and associated in response to a change in [Mg^{2+}], their motions have been studied independently.

2.5.2. Chemomechanical Properties of the F_1-Motor

The rotary motion of ATP synthases was first suggested by Boyer[122] and later supported by the crystal structure of the major part reported by Walkers and co-workers (Figure 16).[123] In 1997, Noji, Yoshida, and co-workers succeeded in direct observation of the rotation of the F_1-motor by means of a microprobe technique.[124] F_1 is a water-soluble protein conjugate, consisting of five different subunits called α, β, γ, δ, and ϵ. In bovine mitochondrial F_1, every three α- and β-subunits are arranged alternately to form a cylindrical heterohexamer having a cavity at its center, which accommodates the γ-subunit, adopting a coiled-coil structure. The conjugate of the α-, β-, and γ-subunits is called a "motor part". F_1 is connected to F_0 via a strap attached to the δ-subunit located in proximity to the motor part. F_1 involves the ϵ-subunit, which guides the γ-subunit into the cavity of F_0. The crystal structure of native bovine mitochondrial F_1, solved in the form of an AMP–PNP (ATP analogue) adduct,[120,123] indicates that all the α-subunits adopt a nearly identical conformation to one another. In contrast, the three β-subunits adopt different conformations depending on the nucleotide-binding mode. The crystal structure also shows that the first β-subunit called β_{TP} bears AMP–PNP in its ATP-binding site, while the second one (β_{DP}) has ADP. The third one (β_E) does not carry nucleotides. The structure of native F_1 is considered a snapshot
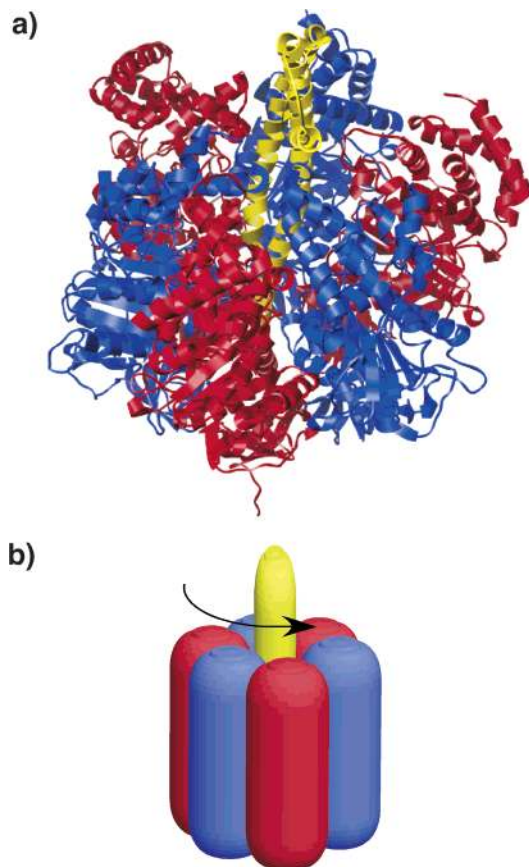
Figure 16. Crystal structure of F_1-ATPase from bovine mitochondria. Red, blue, and yellow segments represent α-, β-, and γ-subunits, respectively. (a) Side view. (b) Schematic structure of the motor part of F_1-ATPase (α-, β-, and γ-subunits).

of the rotating motor. The lower part of the γ-subunit, which adopts a slightly bowing, asymmetric coiled-coil structure, is bent toward β_E; therefore, the carboxy-terminal domain of this β-subunit is swung 30° downward. Thus, β_E adopts an "open" (O) form, whereas β_{TP} and β_{DP} adopt a "closed" (C) form (Figure 17). More recently, the crystal structure of bovine F_1, with all the three ATP-binding sites occupied with nucleotides, has been reported.[121] In this crystalline complex, the two β-subunits, corresponding to β_{TP} and β_{DP} in the above-mentioned native complex, hold Mg-ADP·AlF$_4$ as a phosphate inhibitor at their ATP-binding sites. Their structures are very similar to each other and also to β_{TP} and β_{DP}. The β-subunit, equivalent to β_E, adopts a "half-closed" (C′) conformation and preserves Mg-ADP and sulfate at its ATP-binding site.

On the basis of the above structural features, the following mechanism has been proposed for the rotation of the F_1-motor coupled with a catalytic ATPase cycle (Figure 18). The model involving three β-subunits, β_{TP}–β_{DP}(Pi)–β_E, starts from the C_{TP}–C_{DP}–O state, where β_{TP} and β_{DP}(Pi) (adducts of β-subunits with ATP and ADP·Pi, respectively) are conformationally closed (C_{TP} and C_{DP} states, respectively), while β_E (β-subunit without nucleotides) is open (O state). At first, binding of ATP to β_E takes place, resulting in the transformation of β_E to β_{TP} (C_{TP} state) via an open-to-close conformational transition. Simultaneously, β_{DP}(Pi) in the C_{DP} state undergoes
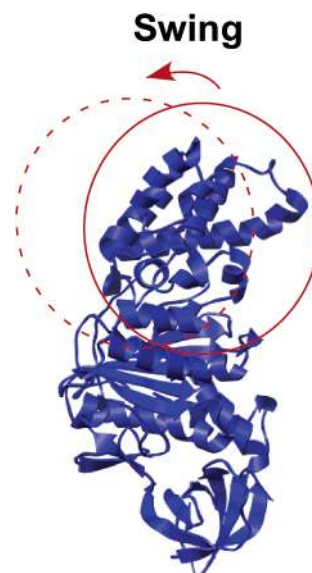

Figure 17. Crystal structure of the closed form of the β-subunit (β_T). The arrow represents conformational change to its open form (β_E).
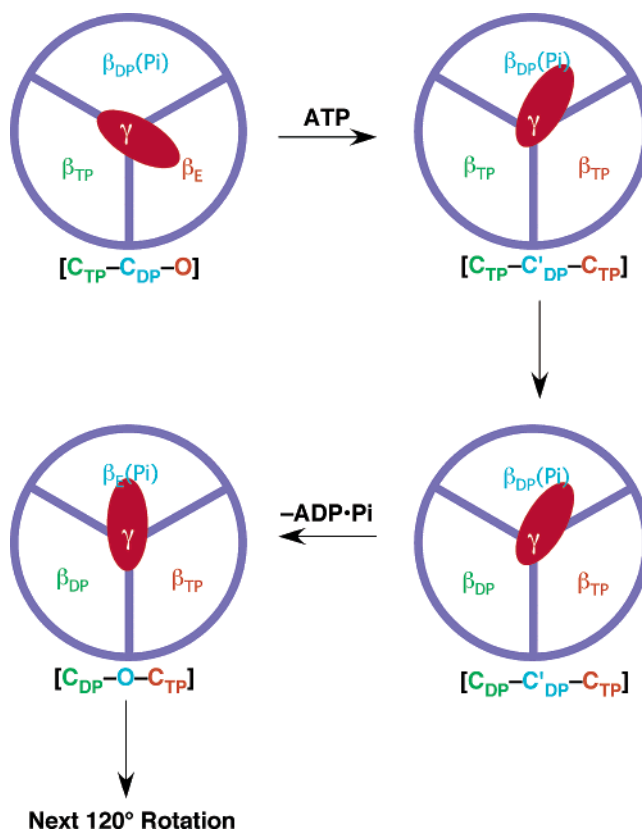

Next 120° Rotation

Figure 18. Schematic representation of the ATPase cycle involving F_1-ATPase. The symbols in brackets represent the states of the corresponding β-subunits: O, open form; C_{TP}, closed form with ATP; C_{DP}, closed form with ADP; $C′_{DP}$, half-closed form with ADP.

a transition to its half-closed form ($C′_{DP}$ state), while the γ-subunit starts to rotate by 90°. In the second step, β_{TP}, upon hydrolysis of its bound ATP, is transformed to β_{DP} (Pi) in the C_{DP} state. Here the model is in the C_{DP}–$C′_{DP}$–C_{TP} state. In the third step, β_{DP}(Pi) in the $C′_{DP}$ state releases ADP and Pi to give β_E in the O state, while the γ-subunit starts to rotate by an additional 30°. After these events, the

model is converted to the $C_{DP}-O-C_{TP}$ state, ready for the next 120° rotation to generate the $O-C_{TP}-C_{DP}$ state. After one more cycle, the model reverts to the initial state ($C_{TP}-C_{DP}-O$) and accomplishes a 360° full rotation. Yoshida and co-workers have reported more details of the rotation mechanism on the basis of single-molecule observation of the F_1-motor immobilized on beads.[125]

2.5.3. Chemomechanical Properties of the F_0-Rotor

As described in the introductory part, ATP synthases produce ATP using ion fluxes. This is a reverse process of the rotary motion of the γ-subunit. Namely, ion fluxes bring about a rotary motion of F_0, which triggers the rotation of the γ-subunit of F_1 (Figure 15). By this rotation, the three β-subunits sequentially change their conformation from the "open" to "half-closed" forms. Then, binding of ADP and Pi takes place, and the β-subunits further change their conformation to the "closed" form. In this way, the 360° full rotation of F_0 results in the formation of three molecules of ATP.

F_0 is a hydrophobic transmembrane protein conjugate, which consists of three subunits called F_0-a, F_0-b, and F_0-c. One F_0-a subunit assembles with two F_0-b subunits to form a strap, while F_0-c subunits construct a circular assembly. In the case of bacterial ATP synthase, F_0 requires a proton flux for rotation. F_0 is embedded in a phospholipid bilayer membrane and includes in its cylindrical cavity the γ-subunit as the shaft of F_1-motor. Although F_0 has not been crystallographically defined yet, the crystal structure of an $F_1 \cdot (F_0\text{-c})_{10}$ conjugate, originating from yeast ATP synthase, has been reported. The crystal structure shows the presence of a circular array of ten F_0-c subunits, which accommodates on its cytoplasmic surface the shaft and ϵ-subunit.[120,126]

Along with the partial crystal structure described above, mutation studies of F_0 have suggested that a periplasmic inlet channel allows protons to enter F_0 and guides them to the Asp61 carboxylate in F_0-c at the $a_1 b_2$ stator interface. When the Asp61 carboxylate is protonated, a positively charged proximal residue of F_0-c moves away from the stator interface to the membrane. After several steps, protons are released from the outlet channel located on the F_1-binding side of the membrane. On the other hand, the γ-subunit in F_1 remains fixed at the top of the circular array of the F_0-c subunits, so that it rotates synchronously with the rotation of F_0.

2.5.4. Application of ATP Synthases

The rotary motions of ATP synthases generate a torque of $80-100$ pN nm^{-1}, indicating a nearly 100% efficiency for the energy conversion of the hydrolysis of ATP into the rotary motion of the F_1-motor.[124,127] Thus, the application of ATP synthases to artificial devices is a fascinating subject.

As a pioneering work, Noji, Yoshida, and co-workers have reported that an actin filament can be rotated by the ATP-fueled rotary motion of the F_1-motor.[124] At first, a biotin unit is attached to the F_1-motor through a cystein residue, which has been introduced by site-directed mutagenesis, and the resulting conjugate is connected to a histidine decamer at the N-terminus of each β-subunit. This engineered F_1-motor is immobilized on a glass plate, whose surface has been covered by Ni^{2+}-nitrilotriacetic acid (Ni-NTA) with a high affinity toward histidine oligomers. Then, a fluorescently labeled, biotinylated actin filament is attached via streptavidin to the γ-subunit of the engineered F_1-motor. Studies with epifluorescence microscopy have shown that the filament rotates in an anticlockwise direction when viewed from the membrane side. The torque under a high load is estimated to be greater than 40 pN nm^{-1}, which is much larger than those with other biological linear motors such as myosins ($3-6$ pN nm^{-1})[128-130] and kinesins (5 pN nm^{-1}).[131,132] Later, Montemagno and co-workers have fabricated arrayed F_1-motors on an engineered surface bearing nanoscale Ni posts, and they have succeeded in rotating the Ni-based nanopropellers attached to the γ-subunit of F_1-motors.[133-135] The rotation of the nanopropellers is initiated by 2 mM ATP, while inhibited by sodium azide. When a F_1-motor having metal-binding sites is used, the rotary motion can be switched on and off reversibly in response to a change in [Zn^{2+}].[136]

Rotary motions of the F_1-motor driven by external forces have been utilized for the synthesis of ATP. For example, Dimroth et al. have reported the synthesis of ATP by a voltage-driven rotation of the F_0-motor using an electrical potential generated with a proteoliposome membrane.[137] Hisabori and co-workers have incorporated a redox-active functionality into a bacterial F_1-motor to control its rotary motion by a redox reaction.[138] Recently, Itoh and co-workers have reported the fabrication of an engineered F_1-motor by attaching a magnetic bead to its γ-subunit, and they have demonstrated the synthesis of ATP by rotating the bead in an appropriate direction using electromagnets.[139]

2.6. Chaperonins

Chaperonins are biological molecular machines, which assist the folding of denatured or newly formed proteins in their cylindrical cavity using the energy derived from ATP hydrolysis.[10] As shown in Figure 19, there are several examples of chaperones whose crystal structures are known.[140-144]

2.6.1. Functional Aspects of Chaperonins

Chaperonins are classified into two groups. Group I contains eubacterial chaperonins exemplified by GroEL originating from *E. coli*, and homologous chaperonins from mitochondria and chloroplasts. These chaperonins have high affinities toward most unfolded proteins both in vivo and in vitro, and they assist protein folding in the presence of co-chaperonins such as GroES. Group II contains eukariyotic chaperonin CCT and chaperonins from archaea. These chaperonins promote protein folding without co-chaperonins. In the eukaryotic cytosol, group II chaperonins are more selective in trapping guest proteins than group I chaperonins.

Most chaperonins adopt cylindrical or hollow spherical shapes. Group I chaperonins possess hydrophobic binding sites at the entrance parts of their cav-
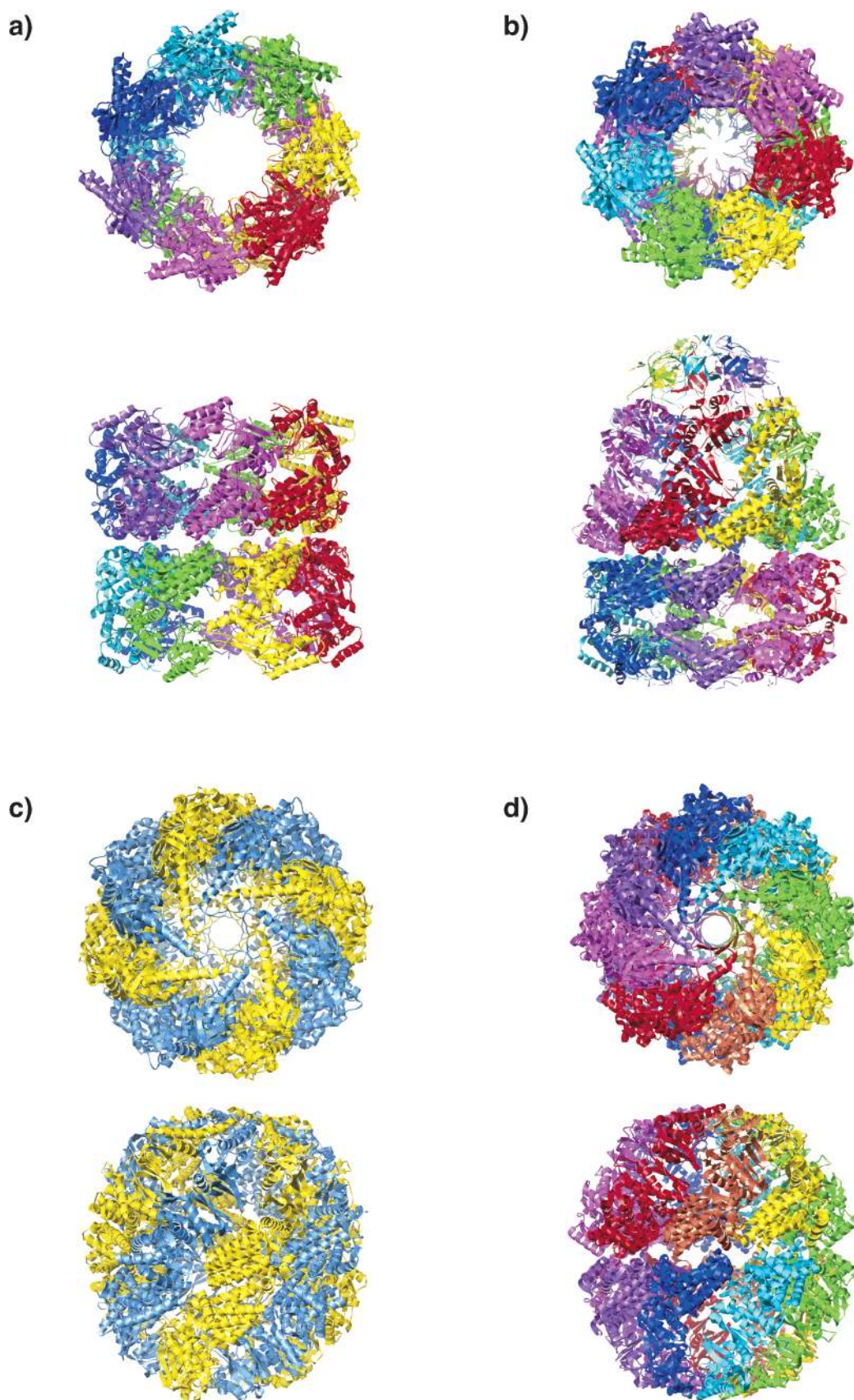
Figure 19. Crystal structures of chaperonins from (a) *E. coli*, (b) *Thermus thermophilus* HB8, (c) *T. acidophilus*, and (d) *Thermococcus* strain KS-1. Upper and lower structures represent top and side views, respectively. Chaperonins a and b belong to group I, while chaperonins c and d belong to group II.

ity.[140,142] These adhesive regions capture unfolded proteins with a hydrophobic surface.[145,146] Such a guest-trapping chaperonin is bound to a co-chapero-

nin, such as GroES, by the assistance of ATP,[146,147] whereupon the guest protein undergoes folding. Upon binding of the second ATP molecule, GroES is de-
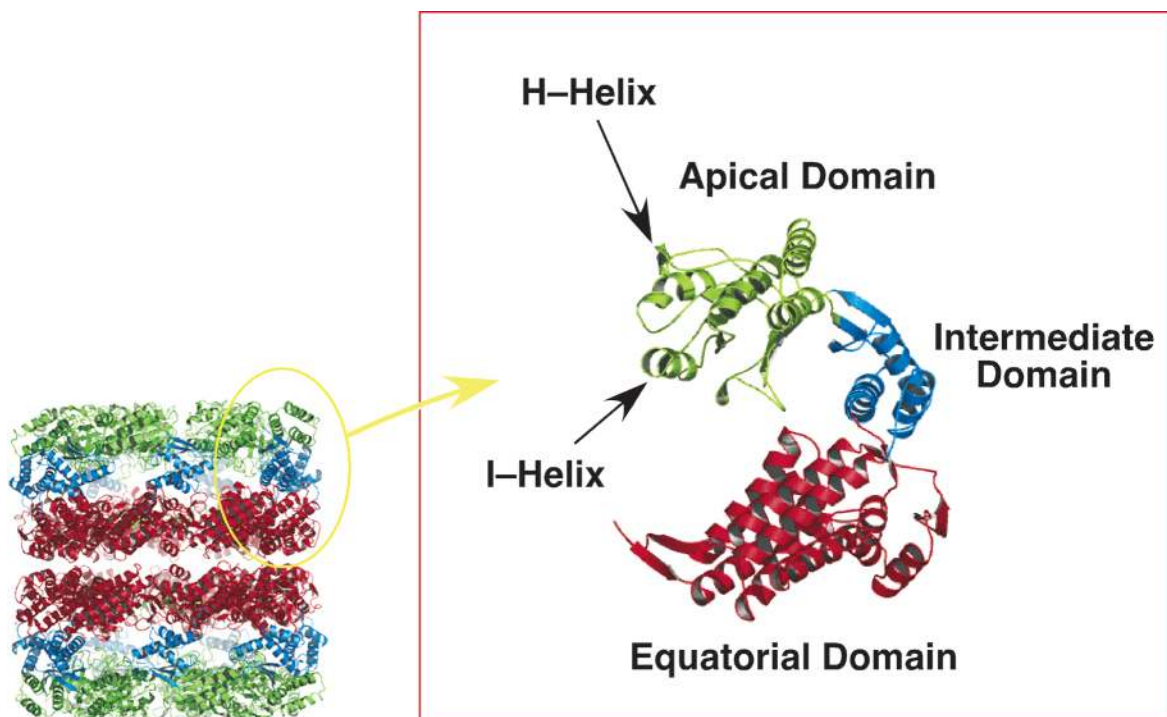
Figure 20. Crystal structure of a subunit of GroEL composed of apical (green), intermediate (blue), and equatorial (red) domains.

tached, and the guest protein is released.[148,149] Thus, the mechanical motions of chaperonins are quite different from those of other biological machines such as myosins, kinesins, and ATP synthases. X-ray crystallography and cryo-electron microscopy have been utilized for the structural understanding of the biological functions of chaperonins.[147,148]

2.6.2. Structure and Chemomechanical Motion of Chaperonin GroEL

GroE proteins, both large (GroEL) and small (GroES), are found in *E. coli*,[150] and the structures of GroEL and the GroEL−GroES conjugate have been crystallographically defined. GroEL is a 14-mer of an identical protein subunit with a molecular mass of 58 kDa, adopting a double-decker architecture formed by the stacking of two supramolecular rings, each consisting of seven protein subunits (Figures 19 and 20).[140,147] The cylindrical cavity, which is surrounded by a 4.6-nm thick protein wall, is 14.6-nm tall and has a diameter of 4.5 nm. GroES, a co-chaperonin, is a bowl-shaped heptamer of a smaller protein subunit, each having a molecular mass of 10 kDa. In the presence of ATP under physiological conditions, GroES is bound to the apical domain of GroEL and caps one of the entrance parts of its cavity.[151]

GroEL consists of three essential parts: an equatorial domain located at the center of the junction of the two heptameric rings, apical domains located at the entrance parts of the cavity, and intermediate domains covalently connected to the apical and equatorial domains (Figure 20). The equatorial domain contains a nucleotide-binding site in proximity to a hinge at the intermediate domain, where amino acid residues D87, D52, K51, and T30 are located and responsible for the hydrolysis of ATP.[142] The inter-

mediate domains do not include binding sites for nucleotides. However, they are considered to play an important role in the allosteric information transfer from one apical domain to the other, since mutations in these domains exert strong effects on the biological activity of GroEL. The apical domains possess binding sites for guest proteins and GroES, where two helices, referred to as the H-helix and the I-helix, exist and form a circular array for capturing unfolded proteins via a hydrophobic interaction.[145]

The binding of ATP to the seven protein subunits in the first heptomeric ring of GroEL is cooperative. The first heptomeric ring with bound ATP exerts a negative allosteric effect on the second heptomeric ring, so that the binding of the next seven ATP molecules is prohibited.[146] This regulation makes the two seven-membered rings asymmetric and allows the ATPase cycle to run sequentially. As soon as the binding of ATP occurs, GroES caps the apical domain of GroEL, located in proximity to the ATP-bound site. Consequently, the capped domain is swung 60° upward and twisted by 90° to contact loops dangling down from the GroES lid (Figure 21). This large mechanical motion results in transforming the guest-bound hydrophobic region of the cavity into an enclosed chamber surrounded by hydrophilic residues. Simultaneously, the guest protein is pushed inside the cavity and undergoes folding in a hydrophilic environment. At this stage, ATP is allowed to bind to the other heptameric ring and gives rise to a large conformational change. This structural change is transmitted via a long-range allosteric interaction to the opposite side capped with GroES.[10,152,153] The refolded guest, along with capping GroES, is then released from the GroEL cavity. Thus, GroEL is a biological molecular machine, which collaborates with GroES and makes use of the ATP-triggered inter-
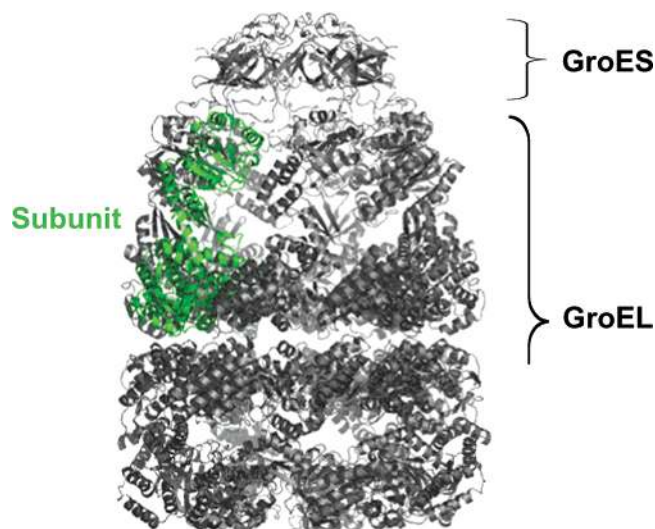
Figure 21. Crystal structure of the GroEL·GroES·ADP$_7$ conjugate, where the two heptomeric rings in GroEL are not identical to each other.

locked motion for the folding of proteins. Recently, kinetic profiles of this folding process have been investigated by means of single-molecule microscopy.[154,155]

2.6.3. Application of Chaperonins

If the mechanical motions of chaperonins can operate for artificial guests, a variety of ATP-responsive intelligent devices could be fabricated.

McMillan and co-workers have fabricated nanodot arrays by hybridizing zinc sulfide-coated cadmium selenide (CdSe−ZnS) nanoparticles with a chaperonin protein originating from *sulfolobus shibatae*.[156,157] This chaperonin is known to form a two-dimensional (2D) crystalline sheet under appropriate conditions.[158] They employed a genetically engineered chaperonin having cystein residues at both entrance parts of the cylindrical cavity. This chaperonin adopts a double-decker architecture, where each ring consists of nine protein subunits. Thus, nine cystein units are circularly arranged along each entrance of the cavity, so that their thiol functionalities can accommodate CdSe−ZnS nanoparticles to form nanodot arrays.

More recently, Aida, Kinbara, and co-workers have succeeded in capturing and ATP-triggered release of cadmium sulfide (CdS) nanoparticles by making use of the mechanical motions of chaperonin proteins (Figure 22).[159] They employed two different chaperonins such as GroEL from *E. coli* and *T.th* cpn from *thermus thermophilus* HB8.[143,160] When a DMF solution of CdS nanoparticles with a mean diameter of 2−3 nm is added to a buffer solution of the chaperonins, the nanoparticles are trapped and stabilized without coagulation. At 4 °C, the nanocomposites with GroEL and *T.th* cpn both preserve the light-emitting activity of the CdS nanocluster for more than one year, whereas the nanoparticles without these chaperonins, under otherwise identical conditions to the above, rapidly undergo aggregation and lose their emission in only 2 h. The presence of CdS nanoparticles in the cavities of these chaperonins has
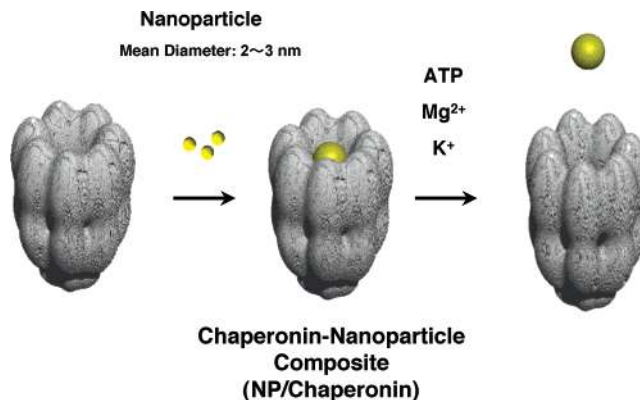

Figure 22. Schematic representation of the capturing and ATP-triggered release of CdS nanoparticles by chaperonin.

been clearly demonstrated by TEM and size-exclusion chromatography, coupled with an absorption/emission dual detector. The thermal stabilities of these nanocomposites are totally dependent on those of the hosting chaperonins, and the nanocomposite with *T.th* cpn, in particular, is stable up to 80 °C and preserves the light-emitting activity. However, by the action of ATP under physiological conditions, the nanoparticles entrapped are readily released from the chaperonins. Analogous to the biological event involved in the chaperonin-mediated protein folding, the ATP-triggered release of the nanoparticles does not take place without Mg^{2+} (nonphysiological conditions). Furthermore, ADP does not induce the release of the nanoparticles. Thus, the release of the nanoparticles takes place most likely by the conformational change of the chaperonin proteins triggered by Mg^{2+}-ATP. This work demonstrates that the biological mechanical motions of chaperonin proteins are applicable to the trapping and release of artificial guests, and indicates a great potential of molecular chaperons for the fabrication of bioresponsive nanodevices.

3. Artificial Molecular Machines

3.1. Molecular Machines with DNA

DNA has been an attractive candidate for the construction of molecular nanodevices, since an appropriate choice of base-pairs guarantees the formation of double strands that allow site-specific displacement of functional units. Along with this advantage, DNA is conductive, and various DNA sequences have been utilized for the fabrication of molecular wires, molecular grids, and other nanoscale molecular objects. Since DNA strands have some conformational isomers, their stimuli-responsive conformational changes are attractive for the fabrication of switching devices.

Seeman and co-workers have reported a DNA-based molecular switch by utilization of a metal ion-triggered transition from B (right-handed) to Z (left-handed) forms (Figure 23).[13] The molecular switch consists of three different DNA strands, which are designed to hybridize together to form a rodlike DNA motif consisting of two double-crossover, antiparallel, odd-number DNA (DAO) domains. The longest strand
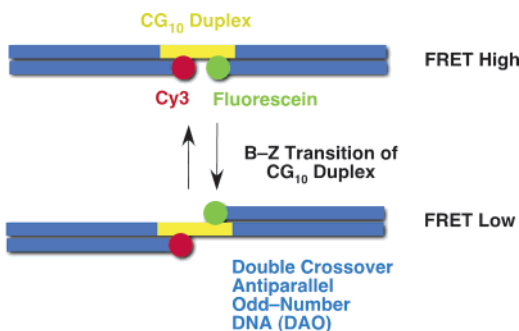
Figure 23. DNA-based twisting molecular machine utilizing a metal ion-triggered transition from B (right-handed) to Z (left-handed) forms.
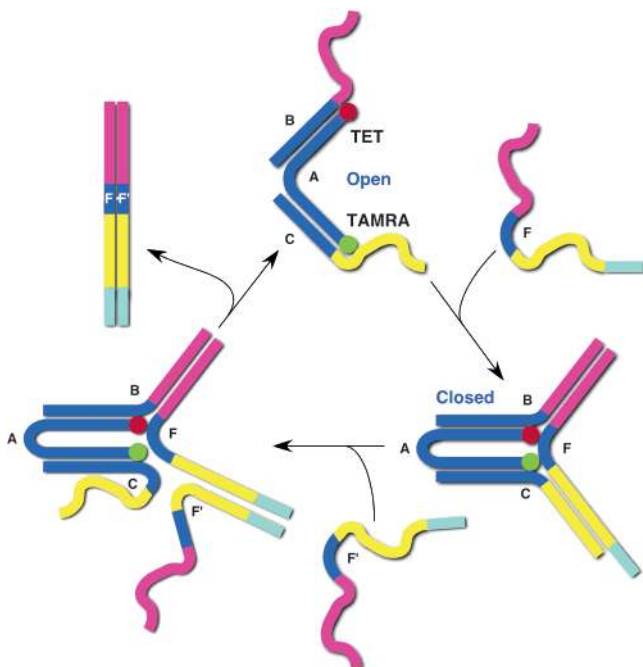

Figure 24. DNA-fueled molecular tweezers composed of a three-stranded DNA (A−C). The "fuel-DNA" (F) has a complementary sequence to the dangling chains linked to the strands B and C. TET = 5′-tetrachlorofluorescein phosphoramidate. TAMRA = carboxytetramethylrhodamine.

contains two, short $d(CG)_{10}$ domains, which are intended to form intramolecularly a duplex region in the middle of the above DNA motif. Fluorescent probes such as fluorescein and sulfoindocarbocyanine (Cy3) are incorporated site-specifically into the DNA motif at the edges of the DAO domains close to the duplex region, so that one can detect the conformational transition at the duplex region by fluorescence resonance energy transfer (FRET) from the former to the latter. In fact, the duplex part is transformed from B to Z upon addition of $Co(NH_3)_6^{3+}$. The transition is accompanied by twisting of the DNA motif at the duplex domain and lowers the FRET efficiency.

Yurke and co-workers have reported a DNA-based molecular machine operative by using DNA as a fuel.[161] The machine consists of a three-stranded DNA (A−C in Figure 24) that looks like tweezers with an "open" geometry. The "fuel-DNA" (F) has a complementary sequence to the dangling chains linked to the strands B and C. Upon addition of the fuel, the two dangling chains are bound to one

molecule of fuel F to form a new DNA double strand. Consequently, the tweezers are transformed to adopt a "closed" geometry. When the single-strand DNA "F′" ("removal-DNA") having a complementary sequence to F is added, F is removed from the tweezers via hybridization with F′ to produce a double-stranded DNA "F·F′" as waste. Thus, the tweezers are able to revert to the "open" geometry. From the sequence of these events, the open−close motion of the molecular tweezers can be considered to be fueled by DNA. A similar strategy has been utilized for the molecular design of the "nanoactuators", which contract and elongate themselves reversibly in response to the "fuel-DNA".[162,163] Yurke et al. call this molecule a "DNA-fueled molecular device". In relation to these studies, Seeman and co-workers have employed a paranemic crossover DNA for the design of a twisting molecular device fueled by DNA. The DNA device utilized in this study has two topoisomers, which are designed to switch from one to the other by hybridization with different DNAs having a complementary sequence.[164] The interconversion induced by such a complementary DNA is accompanied by a twisting motion of the crossover DNA. Tan[165] and Mergny[166] et al. have reported the utilization of a DNA quadruplex−duplex transition for the fabrication of a nanoactuator. In these cases, a DNA molecule, which unimolecularly folds to give a G-quadruplex, is mixed with a single-stranded complementary DNA, whereupon the G-quadruplex is transformed to a heteroduplex. The resultant heteroduplex can be transformed into the initial homoquadruplex by the removal of the hybridized DNA with the "removal-DNA". Since this transition is accompanied by a change in molecular length (5′-3′ distance) between 1.5 and 7 nm with a calculated force of ∼8 pN, the system is referred to as a "DNA-fueled actuator". Balasubramanian et al. have reported a pH-triggered duplex-quadruplex transition by using the oligo-C-based I motif quadruplex,[167] where the actuation can be repeated more than 30 times and generates a calculated force ranging from 10 to 16 pN. Mao et al. have utilized a pH-driven duplex−triplex transition for the design of a DNA nanomachine that undergoes an open−close motion in response to a pH value change.[168] Seeman[169] and Pierce[170] et al. have reported DNA-fueled walking devices, in which a DNA biped can walk along a DNA track. More recent examples include a DNA-fueled molecular gear,[171] in which a pair of DNA circles continuously rolls against each other. Simmel et al. have reported a DNA-based molecular machine that can control the activity of thrombin by DNA-fueled binding and release.[172]

One of the essential problems in DNA-fueled molecular machines is that these systems require sequential addition of the "fuel-DNA" and "removal-DNA" in an alternating manner. If both are added all at once, the "fuel-DNA" is consumed by the preferential hybridization with the "removal-DNA", and the machines would not operate. Turberfield and co-workers have reported the concept of second-generation "fuel-DNA", which is designed to interact selectively with a machine by the introduction of an appropriate protective unit.[173] After the binding with
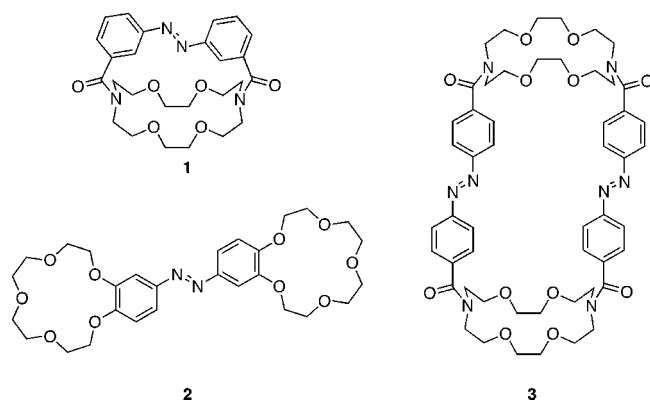
Figure 25. Azobenzene-based molecular machines for selective cation binding.

the machine, "fuel-DNA" automatically releases such a protection and is then removed from the machine by the hybridization with the "removal-DNA" to become a waste. Thus, an automatic operation of the machine is possible as long as initially added "fuel-DNA" remains in the system. Recently, Mao and co-workers have reported such an autonomous DNA motor, where a DNA enzyme is incorporated as a driving part.[174,175] In this system, the enzymic part catalyzes the cleavage of a DNA−RNA chimera substrate. This catalytic process is accompanied by conformational changes of the enzymic part, which trigger an open−close motion of the motor part.

3.2. Molecular Machines with Nonbiological Components

The concept of molecular machines was proposed more than 40 years ago by Feynman, who gave a lecture including some potentials of miniaturized machineries.[176] One of the ultimate goals of research on synthetic molecular machines is to fabricate nanorobots, which perform intelligent functions via programmed motions.

The first-generation molecular machines include photoresponsive azacrown ethers and related compounds (**1**−**3**) reported by Shinkai and co-workers (Figure 25).[177−179] For example, when an azacrown ether including a photoisomerizable azobenzene unit is exposed to UV and visible light,[177] the molecule reversibly changes its conformation, leading to a change in the affinity toward alkali metal ions. When two crown ether units are bridged by an azobenzene unit, the molecule undergoes a butterfly-like motion through a photoinduced isomerization at the azobenzene hinge (**2**).[178,179] Shinkai et al. have extended this approach to molecular systems having two azobenzene units. Examples include a photoresponsive cyclic ionophore containing two azacrown units bridged by two azobenzene units (**3**).[180] During the photoisomerization of this molecule, only the *trans−trans* and *cis−cis* forms are observed, while no *trans−cis* (*cis−trans*) form is detected, suggesting a cooperative isomerization of the two azobenzene units. On the basis of these pioneering works, a variety of synthetic molecular machines have so far been reported, which are based on molecular knots such as catenanes and rotaxanes,[14−17] along with some isomerizable molecules.[181,182]
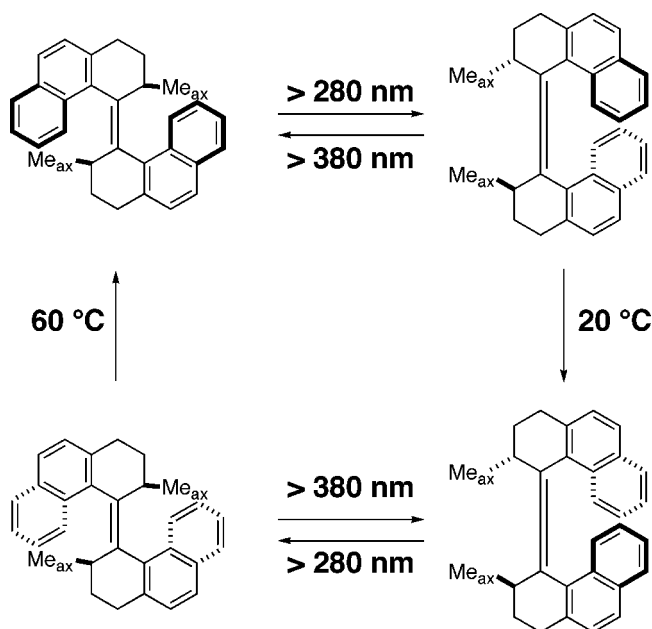

Figure 26. Chiral molecular motor composed of a tetra-substituted alkene. Photoinduced and thermal-induced unidirectional rotation.

To mimic biological molecular machines, one of the most challenging subjects is to realize unidirectional rotary and sliding motions. As described in the above sections, ATP synthases rotate in a counterclockwise direction, while kinesin motors walk along a microtubule from the minus to plus ends. Other important subjects include the integration of multiple interlocked moving components into single molecules for demonstrating highly intelligent motions, as required for molecular robotics. For application to molecular devices, one may also have to consider how to realize tandem actions of a large number of molecules moving on substrates.

3.2.1. Unidirectional Rotary Motions (ATP Synthase and Flagella Mimics)

Some synthetic molecular motors that rotate unidirectionally have been reported.[183,184] Feringa, Harada, and co-workers have succeeded in the design of a chiral molecular motor, which rotates unidirectionally by applying light and heat in a sequential manner.[185] The molecule includes a photoisomerizable tetrasubstituted alkene bearing two large aromatic rings, which has a helical chirality due to a distortion around the C−C double bond, caused by a steric repulsion among the substituents on the alkene part (Figure 26). Upon irradiation at −55 °C with light of wavelength longer than 280 nm, the alkene part undergoes *trans*-to-*cis* isomerization to afford a highly strained *cis* isomer. On heating to 20 °C, the *cis* isomer undergoes a flipping motion with respect to the aromatic rings to give an oppositely twisted helical isomer. When this isomer is again exposed to light of wavelength longer than 280 nm, the *cis* form undergoes isomerization to give a highly strained *trans* isomer, which flips upon heating to 60 °C to return to the initial state. Although the rotation is not continuous but stepwise, the light- and thermal-induced steps, in principle, can be repeated many
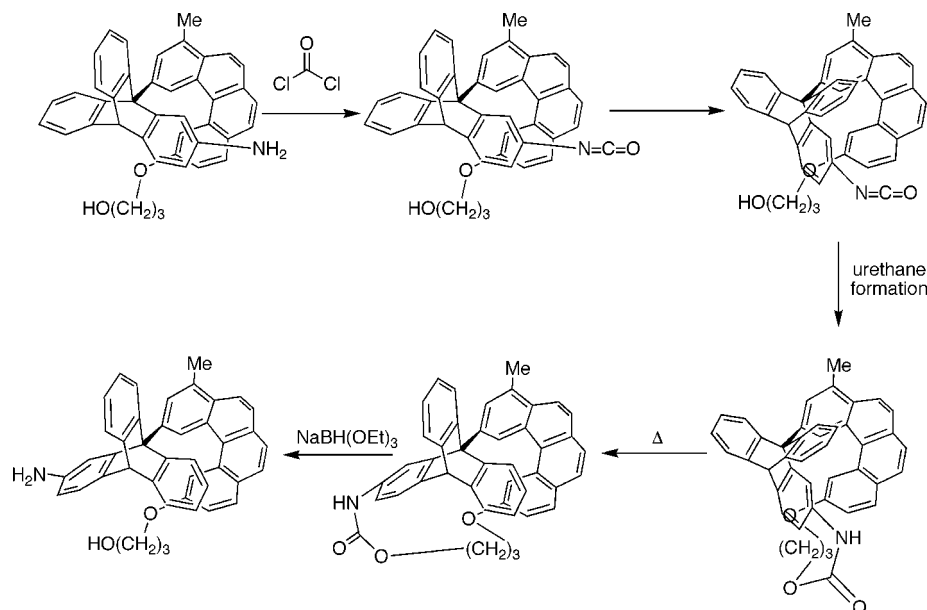
Figure 27. Phosgene-fueled chiral molecular rotor composed of helicene and triptycene.

times, and the molecule may be called a "molecular motor". Later, this prototype molecular motor was improved.[186−188] More recently, Feringa and co-workers integrated a molecular motor into a cholesteric liquid crystalline matrix, where the rotation of the motor switches the helical pitch of the matrix and therefore changes the reflection wavelength of the light.[189]

Kelly and co-workers have reported a chiral molecular rotor by combining an aminotriptycene to a helicene having a hydroxy group. This rotor is chemically fueled by phosgene (Figure 27).[190−192] The triptycene−helicene bond of this molecule rotates, upon addition of phosgene to the amino group, to generate an isocyanate group, which then reacts with the hydroxy group of the helicene part to afford an urethane linkage. The resultant urethane derivative undergoes a partial rotation of the triptycene part to give a thermally stable conformer. Reductive cleavage of the urethane linkage gives a rotational isomer of the initial compound. Although the rotation occurs unidirectionally, a full rotation (360°) has not been achieved.

Leigh and co-workers have reported a catenane-based molecular machine, where two identical small rings are catenated with one large ring bearing four different stations (Figure 28).[193−195] A unidirectional rotation of the small rings along the large ring is achieved by their sequential complexation and de-complexation with the four station parts by applying light, heat, and chemical stimuli. The presence of the two small rings in this catenated system is essential for the unidirectional rotation, as one of the rings eventually blocks the other from undergoing a Brownian movement backward.

With respect to the reality of directed molecular rotation by polarized lights, Hoki and co-workers have reported theoretical calculations on the laser-pulse-induced motion of a small molecule bearing a formyl group as a rotating part.[196−198] In their prediction, unidirectional rotation of the formyl group would occur by irradiation with a laser pulse, al-
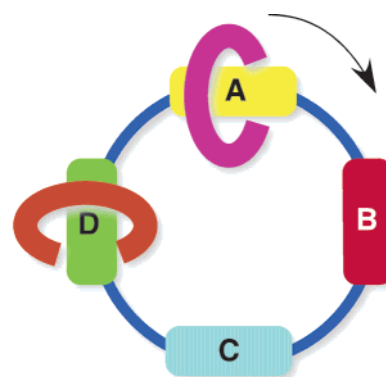

Figure 28. Catenane-based molecular rotor. A unidirectional rotation of the small rings along the large ring is achieved by their sequential complexation and decomplexation with four station parts A−D on exposure to light, heat, and chemical stimuli.

though effects of the chirality of the molecule are expected to be more predominant than those of the polarity of light on the direction of the formyl rotation.

3.2.2. Directed Sliding Motions (Myosin and Kinesin Mimics)

Although there are several molecular systems that realize unidirectional rotations, examples of directional sliding with artificial molecular machines are still rare.

In 1994, Stoddart and co-workers reported, on the basis of their rotaxane synthesis,[199] a pioneering work on stimuli-responsive rotaxanes composed of a macrocyclic ring containing two bipyridinium units and a oligoether shaft having 4,4′-diaminobiphenyl and 4,4′-dialkoxybiphenyl stations (Figure 29). The macrocyclic ring shuttles between these two stations upon redox chemistry of the diaminobiphenyl station or protonation/deprotonation of its amine moieties. This work has elegantly been extended to the design of some stimuli-responsive molecular knots that perform directed sliding motions.[16,17] Recent ex-
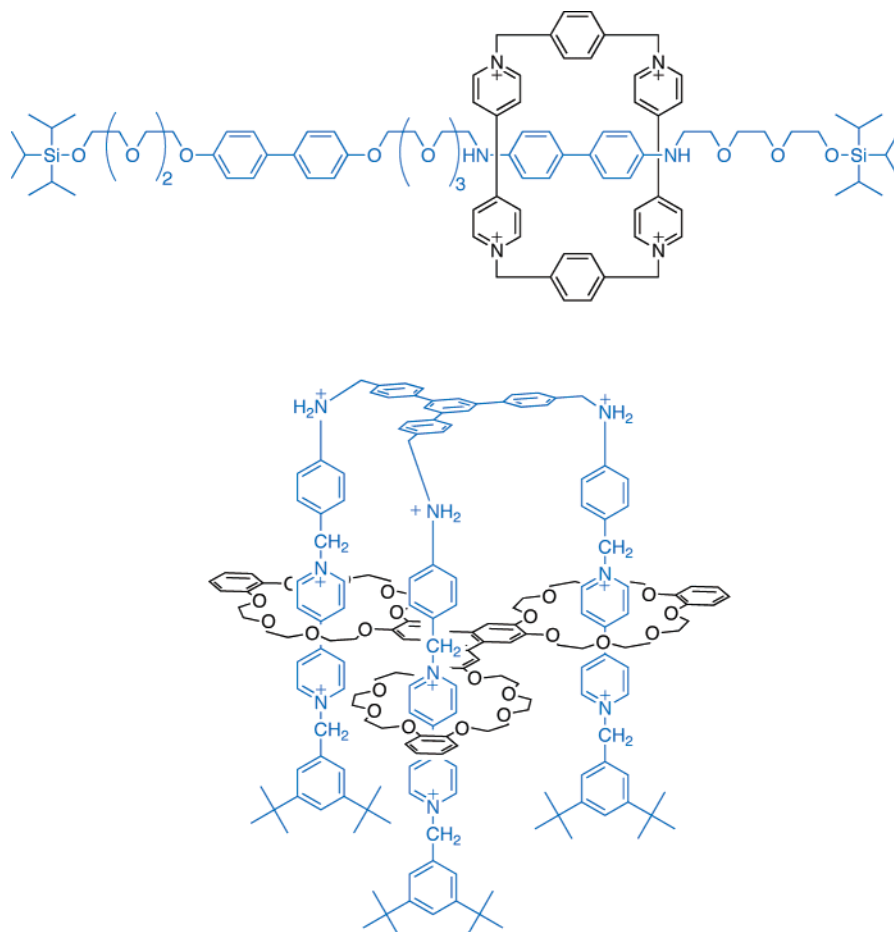
Figure 29. Rotaxane-based molecular shuttle (upper) and an elevator (lower).

amples include a mechanical interlocked system consisting of three rotaxane components, formed by the combination of a triphenylene-based platform with three crown ether units and a triphenylbenzene derivative with three shafts, each having bipyridinium and amine moieties (Figure 29).[200] The rotaxane components undergo sliding motion in response to chemical stimuli. Stoddart et al. refer to this system as a "molecular elevator", since the triphenylene-based platform goes up and down, in response to protonation/deprotonation of the amine moieties, as the result of a tandem motion of the three rotaxane units. When the platform moves from the upper to lower levels, a force up to 200 pN is generated.

Sauvage and co-workers have synthesized artificial molecular muscles that undergo elongation and contraction, by integrating two pseudorotaxane components into a supramolecular complex (Figure 30).[15,201−203] The complex consists of a dimer of a molecule having a phenanthrolin-containing chelating ring and a dimeric phenanthrolin shaft. In the presence of metal ions, each ring is threaded by the shaft of another molecule to form a pseudo-rotaxane. When Cu$^+$ is added, the complex adopts an "extended" form, where the phenanthroline units in the rings and shafts both coordinate to Cu$^+$. When Cu$^+$ is removed and then Zn^{2+} is added to this system, the phenanthroline units in the rings and the terpyridine units in the shafts both coordinate to Zn^{2+},

so that the entire molecule turns to adopt a "contracted" form. On repetition of this sequential complexation/decomplexation cycle, the molecule undergoes elongation and contraction reversibly, and the system is regarded as an artificial myosin mimic. The bis-rotaxane compound, upon transition from its extended to contracted forms, is estimated to change from 83 to 65 Å in length. The extent of this change is roughly comparable to those of natural muscles (∼27%).

Rowan, Nolte, and co-workers have proposed that a manganese porphyrin-appended toroidal catalyst can mimic processive enzymes in epoxidation of polybutadiene (Figure 31).[204,205] When the open face of the toroidal catalyst is blocked by the coordination of a bulky ligand such as 4-*tert*-butylpyridine to the manganese porphyrin, the catalyst is bound to polybutadiene to form a pseudo-rotaxane. The toroidal catalyst is expected to preserve the rotaxane structure and epoxidize olefinic double bonds processively by walking from one end of the polybutadiene chain to the other. Although the proof for the unidirectional movement of the catalyst awaits further studies, the turnover number of this supramolecular catalytic reaction (7−21) is almost comparable to that for the reaction mediated by cytochrome P-450 (0.1−60).[206,207]

3.2.3. Multiple Interlocked Motions

In daily life, we utilize many machines, most of which include several moving parts that perform
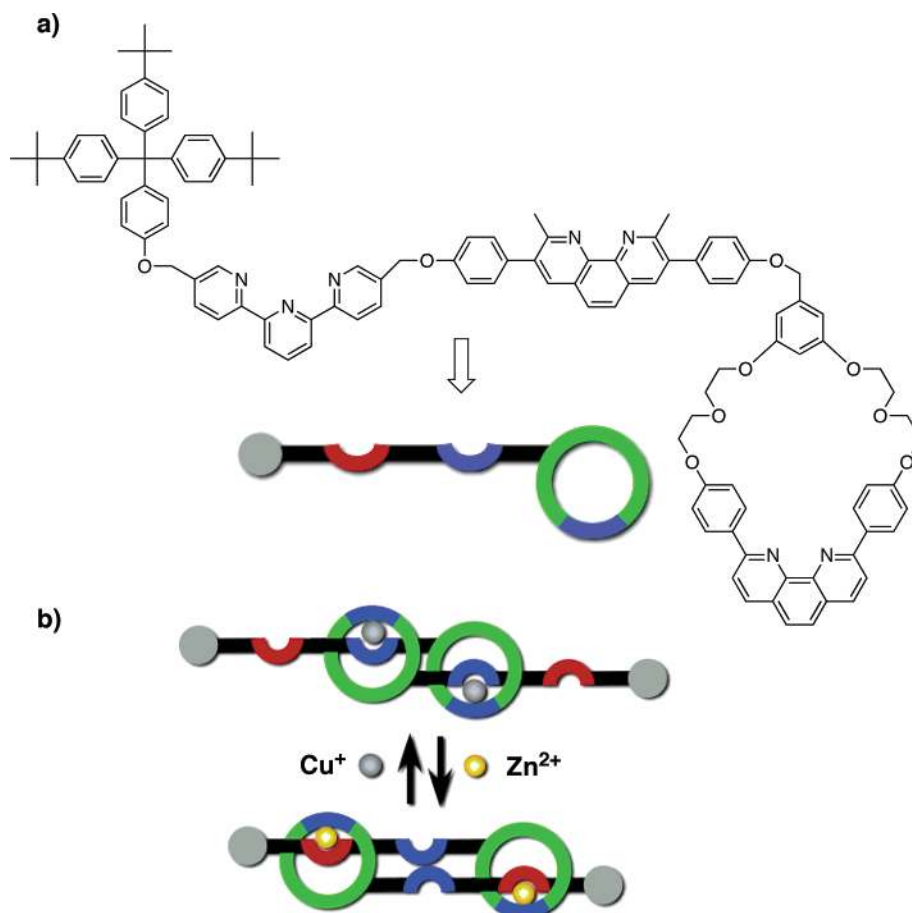
Figure 30. Rotaxane-based molecular muscle operative by redox-driven complexation/decomplexation with metal ions.
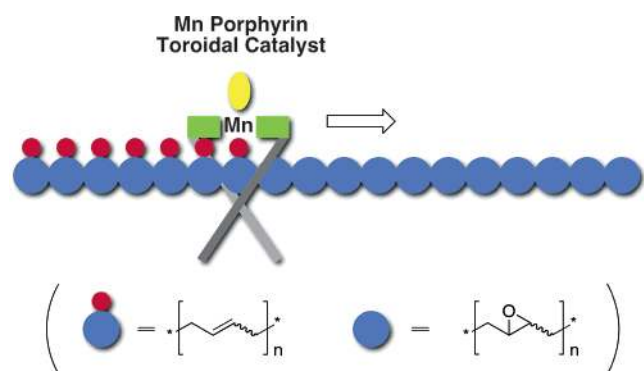

Figure 31. Manganese porphyrin-appended linear-motor catalyst for the epoxidation of polybutadiene. The epoxidation on the open face of the catalysts is suppressed by the coordination with a bulky ligand (yellow oval).

different motions. Upon connection of those moving parts, their different motions are interlocked to give desired outputs. For example, in engines, a piston action is translated into a rotary motion. A molecular machine that performs internal conversion of moving mechanisms has recently been developed.

Kinbara, Aida, and co-workers have reported photoresponsive molecular scissors containing azobenzene and ferrocene units, where a photodriven contracting/elongating motion of the azobenzene unit is translated into a pivotal motion at the interlocked ferrocene unit and then to an open—close motion of the blade parts connected to the ferrocene unit

(Figure 32).[208] Since the ferrocene unit is chiral, one can clearly observe a pivotal motion at the ferrocene unit by a change in the circular dichroism spectral profile of the enantiomers in response to ultraviolet and visible lights. Incorporation of some functional units into the chiral scissors would give a new class of photoresponsive molecular machines.

3.2.4. Coherent or Tandem Directed Motions of Assembled Molecules

As described above, through extensive studies on the behavior of individual molecules in solution, a variety of molecular and supramolecular systems have been found to perform directional motions. However, for the application of molecular machines in practical use, it is crucial to realize coherent and/ or tandem directed motions of such molecules aligned on substrate surfaces.

Ichimura and co-workers have reported a light-controlled motion of a liquid droplet on a photoresponsive surface.[209] In this study, a droplet such as water or olive oil is put on a silica surface covered with a monolayer of a calixarene bearing four 4-octylazobenzene moieties at one of the rims of its cyclic skeleton (Figure 33). Photoirradiation gives rise to a gradient in surface free energy due to the isomerization of the azobenzene groups on the surface, leading to a directional motion of the droplet. The direction and velocity of the droplet motion are tunable by varying the direction and steepness of the gradient
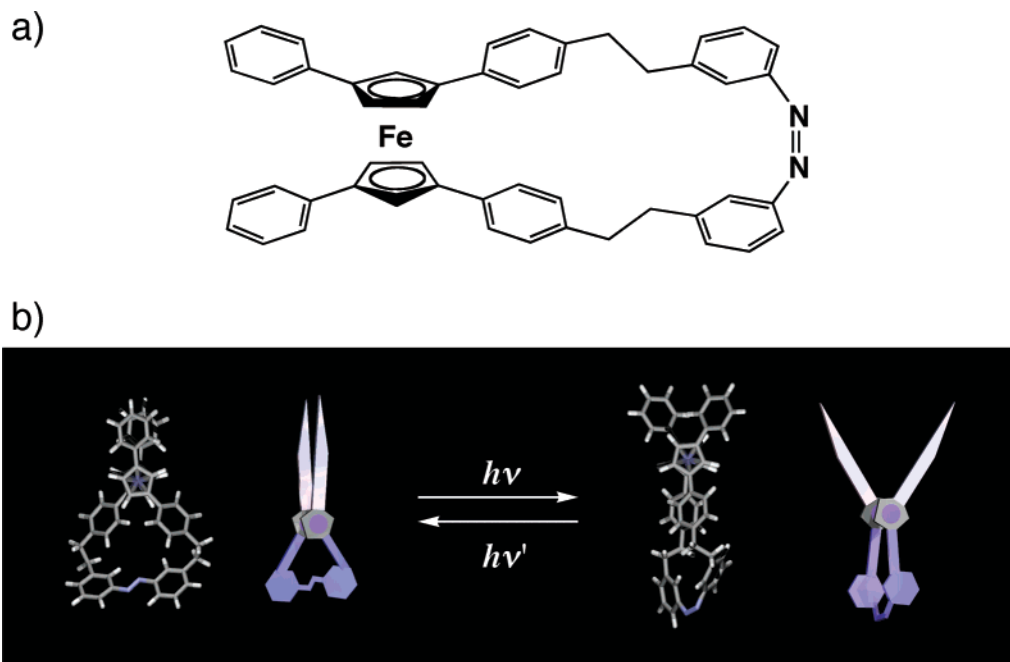
a)

b)

Figure 32. Light-driven chiral molecular scissors composed of azobenzene and ferrocene units. (a) Structure and (b) schematic representation of its light-driven open−close motion.
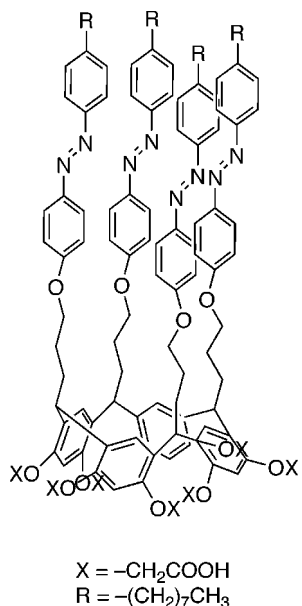

X = −CH₂COOH
R = −(CH₂)₇CH₃

Figure 33. Structure of a photoresponsive calixarene deposited on a silica surface.

in light intensity. This is a physical approach to the unidirectional movement of macroscopic objects.

Sheiko, Möller, and Percec have observed persistent motion of small clusters of monodendron-jacketed linear chains on a surface of highly oriented pyrolytic graphite (HOPG).[210] The motion can be ascribed to contraction/elongation events of the polymer backbone due to the desorption/adsorption of the densely grafted side groups. When cylindrically shaped molecules adsorb to a flat substrate surface, their conformations are controlled by a steric repulsion between the adsorbed side groups (or chains). Owing to the very high grafting density, the backbone gets extended. However, it contracts again if some of the side groups eventually desorb. It is believed that the

coherent contraction/extension cycles of neighboring molecules in the cluster give rise to a translational motion. The large persistence length or directionality of the motion is ascribed to an epitaxial alignment of the cylindrical molecules along the crystallographic directions of the graphite lattice. The controlled adsorption of side chains in brushlike molecules provides a new tool for triggering the motion of hyperbranched macromolecules as individual species as well as collective sliding of monolayer films on surfaces. Recently, Sheiko and Matyjaszewski have reported molecular visualization of poly(butyl acrylate) cylindrical brushes as they spread on a solid substrate.[211] These experiments make it possible to follow the fluid transport on the molecular level, thereby enabling microscopic understanding of the underlying physical mechanism.

Ikeda and co-workers have shown that a film of a cross-linked liquid-crystal network containing an azobenzene chromophore serves as a photoresponsive actuator sheet, which can be repeatedly bent along any chosen direction by using linearly-polarized ultraviolet and visible light.[212] In the film, the azobenzene units in each liquid crystalline domain are unidirectionally aligned. When the film is exposed to a linearly-polarized light, the azobenzene units parallel to the polarized light are selectively excited to give the corresponding isomers. Since photoisomerized domains give rise to the macroscopic contraction of their volume, bending of the film takes place along a direction of the polarized light. In contrast, if the azobenzene units in a single liquid crystalline domain are not aligned, such a macroscopic motion of the film cannot be expected.

Tabe and Yokoyama have reported a coherent collective precession of chiral rodlike molecules in a liquid crystalline monolayer driven by the trans-membrane transfer of water molecules.[213] When a
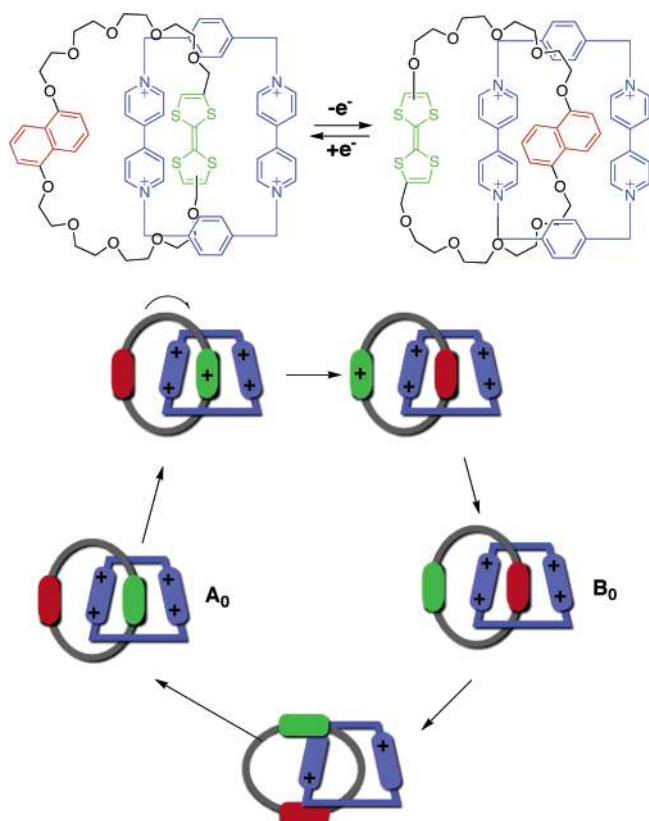
Figure 34. Schematic representation of a catenane-based switching device for electric circuits. Counteranions (PF_6^-) are omitted for clarity.

rodlike molecule with a chiral epoxide group is placed on glycerol to from a monolayer, it is tilted toward the monolayer surface to allow precession. Studies with reflected-type polarizing microscopy have shown a characteristic oscillation pattern of the reflection, suggesting a coherent rotary motion of a number of the molecules in each domain. Such a rotary motion driven by a transmembrane flux is reminiscent of the mechanical motion of F_0-ATPase.

3.2.5. Molecular Machinery for Devices

An exploration has just started for the device application of molecular machines that can realize directed motions. An interesting issue is whether the behaviors of these molecules on dry substrate surfaces are similar to those in solution.[214]

Stoddart, Heath, and co-workers have reported a [2]catenane-based electronic switching device consisting of a monolayer of a [2]catenane placed on an n-type polycrystalline silicon bottom electrode and covered by a metallic top electrode (Figure 34).[215,216] The [2]catenane is composed of two macrocyclic rings, one containing two electron-deficient bipyridinium moieties ($2Bpy^{2+}$) and the other carrying 1,5-dialkoxynaphthalene and tetrathiafulvalene (TTF) moieties. While the $2Bpy^{2+}$ ring in MeCN is initially located at the electron-rich TTF moiety (A_0), it moves onto the dialkoxynaphthalene moiety upon oxidation of the TTF unit, and it returns to the initial place upon reduction of the oxidized TTF. In contrast, when sandwiched by the electrodes, the catenane shows a hysteretic behavior, where the $2Bpy^{2+}$ ring does not

return, unless it is reduced, but remains on the dialkoxynaphthalene moiety even after the oxidized TTF unit is reduced to a neutral state. Thus, in this device configuration, there are two different neutral states A_0 and B_0 for the catenane in terms of the topology of the $2Bpy^{2+}$ ring. Stoddart et al. have also reported that these two neutral states can be switched by applying voltages of $+2$ and -2 V. Since one of the neutral species (B_0) is electroconductive but the other (A_0) is an insulator, the catenane behaves like a switching device for electric circuits.

4. Conclusions

Nanotechnology is expected to contribute to "lab-on-a-chip" technologies, where miniaturized electronic devices and mechanically movable parts are assembled on a single chip to efficiently perform required tasks. Through the present review article, one may recognize the substantial advances in the mechanistic understanding of moving proteins in biological systems and molecular design of second-generation artificial molecular machines. Although biological and artificial molecular machines are potential candidates as components for miniaturized devices, both possess certain advantages and disadvantages. For example, biomolecular nanomachines mostly operate under wet conditions, require ATP as the fuel or ion fluxes to operate, and are thermally unstable. However, they can provide directed or programmed motions. In contrast, although most artificial molecular machines reported so far are less sophisticated and cannot achieve complicated motions, they are more robust and may be operative under a variety of conditions. One of the attractive approaches toward the realization of molecular machinery would be to hybridize biological and artificial movable components. Although seamless integration and proper alignment of those movable parts needs a lot of hard work, their complimentary role may lead to a higher durability and even more sophisticated performances. The dream of molecular robotics might come true within the next 10 to 20 years. For example, a light-tracking, self-propelled molecular robot that carries cargo to a designated point might be realistic.

5. Acknowledgment

6. References

(1) *Molecular Motors*; Schliwa, M., Ed.; Wiley-VCH: Weinheim, 2003.
(2) Vallee, R. B.; Hook, P. *Nature* **2003**, *421*, 701.
(3) Tyreman, M. J. A.; Molloy, J. E. *IEE Proc.: Nanobiotechnology* **2003**, *150*, 95.
(4) Schliwa, M.; Woehlke, G. *Nature* **2003**, *422*, 759.
(5) Ball, P. *Nanotechnology* **2002**, *13*, R15.
(6) Namba, K.; Vonderviszt, F. *Q. Rev. Biophys.* **1997**, *30*, 1.
(7) Yoshida, M.; Muneynki, E.; Hisabori, T. *Nat. Rev. Mol. Cell Biol.* **2001**, *2*, 669.
(8) Boyer, P. D. *Nature* **1999**, *402*, 247.
(9) Stock, D.; Leslie, A. G. W.; Walker, J. E. *Science* **1999**, *286*, 1700.
(10) Saibil, H. R.; Ranson, N. A. *Trends Biochem. Sci.* **2002**, *27*, 627.

(11) Von Hippel, P. H.; Delagoutte, E. *Cell* **2001**, *104*, 177.
(12) Spirin, A. S. *FEBS Lett.* **2002**, *514*, 2.
(13) Mao, C.; Sun, W.; Shen, Z.; Seeman, N. C. *Nature* **1999**, *397*, 144.
(14) Kelly, T. R. *Molecular Devices and Machines: A Journey into the Nanoworld*; Balzani, V., Venturi, M., Credi, A., Eds.; Wiley-VCH: Weinheim, 2003.
(15) Collin, J.-P.; Dietrich-Buchecker, C.; Gavina, P.; Jimenez-Molero, M. C.; Sauvage, J.-P. *Acc. Chem. Res.* **2001**, *34*, 477.
(16) Balzani, V.; Credi, A.; Raymo, F. M.; Stoddart, J. F. *Angew. Chem., Int. Ed.* **2000**, *39*, 3348.
(17) Pease, A. R.; Jeppesen, J. O.; Stoddart, J. F.; Luo, Y.; Collier, C. P.; Heath, J. R. *Acc. Chem. Res.* **2001**, *34*, 433.
(18) Kabsch, W.; Mannherz, H. G.; Suck, D.; Pai, E. F.; Holmes, K. C. *Nature* **1990**, *347*, 37.
(19) Holmes, K. C.; Popp, D.; Gebhard, W.; Kabsch, W. *Nature* **1990**, *347*, 44.
(20) Mermall, V.; Post, P. L.; Mooseker, M. S. *Science* **1998**, *279*, 527.
(21) Sellers, J. R. *Biochim. Biophys. Acta* **2000**, *1496*, 3.
(22) Berg, J. S.; Powell, B. C.; Cheney, R. E. *Mol. Biol. Cell* **2001**, *12*, 780.
(23) De La Cruz, E. M.; Ostap, E. M. *Curr. Opin. Cell Biol.* **2004**, *16*, 61.
(24) Mihalyi, E.; Szent-Gyorgyi, A. G. *J. Biol. Chem.* **1953**, *201*, 189.
(25) Kühne, W. *Leipzig, Verlag von Wilhelm Engelmann* **1864**.
(26) Rayment, I.; Rypniewski, W. R.; Schmidt-Baese, K.; Smith, R.; Tomchick, D. R.; Benning, M. M.; Winkelmann, D. A.; Wesenberg, G.; Holden, H. M. *Science* **1993**, *261*, 50.
(27) Rayment, I.; Holden, H. M.; Whittaker, M.; Yohn, C. B.; Lorenz, M.; Holmese, K. C.; Milligan, R. A. *Science* **1993**, *261*, 58.
(28) Holmes, K. C. *Curr. Biol.* **1997**, 7, R112.
(29) Dominguez, R.; Freyzon, Y.; Trybus, K. M.; Cohen, C. *Cell* **1998**, *94*, 559.
(30) Houdusse, A.; Kalabokis, V. N.; Himmel, D.; Szent-Gyorgyi, A. G.; Cohen, C. *Cell* **1999**, *97*, 459.
(31) Reedy, M. C. *J. Cell Sci.* **2000**, *113*, 3551.
(32) Shih, W. M.; Gryczynski, Z.; Lakowicz, J. R.; Spudich, J. A. *Cell* **2000**, *102*, 683.
(33) Irving, M.; Piazzesi, G.; Lucii, L.; Sun, Y.-B.; Harford, J. J.; Dobbie, I. M.; Ferenczi, M. A.; Reconditi, M.; Lombardi, V. *Nat. Struct. Biol.* **2000**, 7, 482.
(34) Himmel, D. M.; Gourinath, S.; Reshetnikova, L.; Shen, Y.; Szent-Gyorgyi, A. G.; Cohen, C. *Proc. Natl. Acad. Sci. U.S.A.* **2002**, *99*, 12645.
(35) Gourinath, S.; Himmel, D. M.; Brown, J. H.; Reshetnikova, L.; Szent-Gyorgyi, A. G.; Cohen, C. *Structure* **2003**, *11*, 1621.
(36) Ait-Haddou, R.; Herzog, W. *Cell Biochem. Biophys.* **2003**, *38*, 191.
(37) Yanagida, T.; Kitamura, K.; Tanaka, H.; Iwane, A. H.; Esaki, S. *Curr. Opin. Cell Biol.* **2000**, *12*, 20.
(38) Yanagida, T.; Iwane, A. H. *Proc. Natl. Acad. Sci. U.S.A.* **2000**, *97*, 9357.
(39) Veigel, C.; Coluccio, L. M.; Jontes, J. D.; Sparrow, J. C.; Milligan, R. A.; Molloy, J. E. *Nature* **1999**, *398*, 530.
(40) Kitamura, K.; Tokunaga, M.; Iwane, A. H.; Yanagida, T. *Nature* **1999**, *397*, 129.
(41) Mehta, A. D.; Rief, M.; Spudich, J. A.; Smith, D. A.; Simmons, R. M. *Science* **1999**, *283*, 1689.
(42) Ishii, Y.; Ishijima, A.; Yanagida, T. *Trends Biotechnol.* **2001**, *19*, 211.
(43) Morel, J. E.; D'Hahan, N. *Biochim. Biophys. Acta* **2000**, *1474*, 128.
(44) Bunk, R.; Klinth, J.; Rosengren, J.; Nicholls, I.; Tagerud, S.; Omling, P.; Mansson, A.; Montelius, L. *Microelectron. Eng.* **2003**, *67−68*, 899.
(45) Kron, S. J.; Spudich, J. A. *Proc. Natl. Acad. Sci. U.S.A.* **1986**, *83*, 6272.
(46) Sase, I.; Miyata, H.; Ishiwata, S.; Kinosita, K., Jr. *Proc. Natl. Acad. Sci. U.S.A.* **1997**, *94*, 5646.
(47) Nicolau, D. V.; Suzuki, H.; Mashiko, S.; Taguchi, T.; Yoshikawa, S. *Biophys. J.* **1999**, *77*, 1126.
(48) Bunk, R.; Klinth, J.; Montelius, L.; Nicholls, I. A.; Omling, P.; Tagerud, S.; Månsson, A. *Biochem. Biophys. Res. Commun.* **2003**, *301*, 783.
(49) Månsson, A.; Sundberg, M.; Balaz, M.; Bunk, R.; Nicholls, I. A.; Omling, P.; Tagerud, S.; Montelius, L. *Biochem. Biophys. Res. Commun.* **2004**, *314*, 529.
(50) Tanaka, T.; Yamasaki, H.; Tsujimura, N.; Nakamura, N.; Matsunaga, T. *Mater. Sci. Eng., C* **1997**, *C5*, 121.
(51) Vale, R. D. *Cell* **2003**, *112*, 467.
(52) Mehta, A. D.; Rock, R. S.; Rief, M.; Spudich, J. A.; Mooseker, M. S.; Cheney, R. E. *Nature* **1999**, *400*, 590.
(53) Sakamoto, T.; Amitani, T.; Yokota, E.; Ando, T. *Biochem. Biophys. Res. Commun.* **2000**, *272*, 586.
(54) Walker, M. L.; Burgess, S. A.; Sellers, J. R.; Wang, F.; Hammer, J. A., III; Trinick, J.; Knight, P. J. *Nature* **2000**, *405*, 804.
(55) Yildiz, A.; Forkey, J. N.; McKinney, S. A.; Ha, T.; Goldman, Y. E.; Selvin, P. R. *Science* **2003**, *300*, 2061.
(56) Vale, R. D. *J. Cell Biol.* **2003**, *163*, 445.
(57) Forkey, J. N.; Quinlan, M. E.; Alexander Shaw, M.; Corrie, J. E. T.; Goldman, Y. E. *Nature* **2003**, *422*, 399.
(58) Asokan, S. B.; Jawerth, L.; Carroll, R. L.; Cheney, R. E.; Washburn, S.; Superfine, R. *Nano Lett.* **2003**, *3*, 431.
(59) Vale, R. D.; Reese, T. S.; Sheetz, M. P. *Cell* **1985**, *42*, 39.
(60) Nogales, E.; Whittaker, M.; Milligan, R. A.; Downing, K. H. *Cell* **1999**, *96*, 79.
(61) Lowe, J.; Li, H.; Downing, K. H.; Nogales, E. *J. Mol. Biol* **2001**, *313*, 1045.
(62) Miki, H.; Setou, M.; Kaneshiro, K.; Hirokawa, N. *Proc. Natl. Acad. Sci. U.S.A.* **2001**, *98*, 7004.
(63) Hirokawa, N.; Noda, Y.; Okada, Y. *Curr. Opin. Cell Biol.* **1998**, *10*, 60.
(64) Nakagawa, T.; Tanaka, Y.; Matsuoka, E.; Kondo, S.; Okada, Y.; Noda, Y.; Kanai, Y.; Hirokawa, N. *Proc. Natl. Acad. Sci. U.S.A.* **1997**, *94*, 9654.
(65) Kozielski, F.; Sack, S.; Marx, A.; Thormahlen, M.; Schonbrunn, E.; Biou, V.; Thompson, A.; Mandelkow, E. M.; Mandelkow, E. *Cell* **1997**, *91*, 985.
(66) Kikkawa, M.; Okada, Y.; Hirokawa, N. *Cell* **2000**, *100*, 241.
(67) Rayment, I. *Structure* **1996**, *4*, 501.
(68) Hirokawa, N.; Pfister, K. K.; Yorifuji, H.; Wagner, M. C.; Brady, S. T.; Bloom, G. S. *Cell* **1989**, *56*, 867.
(69) Kikkawa, M.; Sablin, E. P.; Okada, Y.; Yajima, H.; Fletterick, R. J.; Hirokawa, N. *Nature* **2001**, *411*, 439.
(70) Svoboda, K.; Schmidt, C. F.; Schnapp, B. J.; Block, S. M. *Nature* **1993**, *365*, 721.
(71) Okada, Y.; Higuchi, H.; Hirokawa, N. *Nature* **2003**, *424*, 574.
(72) Stewart, R. J.; Thaler, J. P.; Goldstein, L. S. *Proc. Natl. Acad. Sci. U.S.A.* **1993**, *90*, 5209.
(73) Hancock, W. O.; Howard, J. *Proc. Natl. Acad. Sci. U.S.A.* **1999**, *96*, 13147.
(74) Schief, W. R.; Howard, J. *Curr. Opin. Cell Biol.* **2001**, *13*, 19.
(75) Kojima, H.; Muto, E.; Higuchi, H.; Yanagida, T. *Biophys. J.* **1997**, *73*, 2012.
(76) Schnitzer, M. J.; Block, S. M. *Nature* **1997**, *388*, 386.
(77) Coy, D. L.; Wagenbach, M.; Howard, J. *J. Biol. Chem.* **1999**, *274*, 3667.
(78) Howard, J. *Annu. Rev. Physiol.* **1996**, *58*, 703.
(79) Hua, W.; Chung, J.; Gelles, J. *Science* **2002**, *295*, 844.
(80) Asbury, C. L.; Fehr, A. N.; Block, S. M. *Science* **2003**, *302*, 2130.
(81) Yildiz, A.; Tomishige, M.; Vale, R. D.; Selvin, P. R. *Science* **2004**, *303*, 676.
(82) Hess, H.; Vogel, V. *Rev. Mol. Biotechnol.* **2001**, *82*, 67.
(83) Hess, H.; Bachand, G. D.; Vogel, V. *Chem. Eur. J* **2004**, *10*, 2110.
(84) Howard, J.; Hudspeth, A. J.; Vale, R. D. *Nature* **1989**, *342*, 154.
(85) Block, S. M.; Goldstein, L. S.; Schnapp, B. J. *Nature* **1990**, *348*, 348.
(86) Vale, R. D.; Funatsu, T.; Pierce, D. W.; Romberg, L.; Harada, Y.; Yanagida, T. *Nature* **1996**, *380*, 451.
(87) Dennis, J. R.; Howard, J.; Vogel, V. *Nanotechnology* **1999**, *10*, 232.
(88) Hess, H.; Matzke, C. M.; Doot, R. K.; Clemmens, J.; Bachand, G. D.; Bunker, B. C.; Vogel, V. *Nano Lett.* **2003**, *3*, 1651.
(89) Hiratsuka, Y.; Tada, T.; Oiwa, K.; Kanayama, T.; Uyeda, T. Q. P. *Biophys. J.* **2001**, *81*, 1555.
(90) Stracke, R.; Böhm, K. J.; Burgold, J.; Schacht, H.-J.; Unger, E. *Nanotechnology* **2000**, *11*, 52.
(91) Limberis, L.; Magda, J. J.; Stewart, R. J. *Nano Lett.* **2001**, *1*, 277.
(92) Brown, T. B.; Hancock, W. O. *Nano Lett.* **2002**, *2*, 1131.
(93) Limberis, L.; Stewart, R. J. *Nanotechnology* **2000**, *11*, 47.
(94) Böhm, K. J.; Stracke, R.; Muhlig, P.; Unger, E. *Nanotechnology* **2001**, *12*, 238.
(95) Bachand, G. D.; Rivera, S. B.; Boal, A. K.; Gaudioso, J.; Liu, J.; Bunker, B. C. *Nano Lett.* **2004**, *4*, 817.
(96) Hess, H.; Howard, J.; Vogel, V. *Nano Lett.* **2002**, *2*, 1113.
(97) Hess, H.; Clemmens, J.; Qin, D.; Howard, J.; Vogel, V. *Nano Lett.* **2001**, *1*, 235.
(98) Dantzig, J. A.; Higuchi, H.; Goldman, Y. E. *Methods Enzymol.* **1998**, *291*, 307.
(99) Taylor, H. C.; Holwill, M. E. J. *Nanotechnology* **1999**, *10*, 237.
(100) Vallee, R. B.; Hook, P. *Nature* **2003**, *421*, 701.
(101) Vallee, R. B.; Williams, J. C.; Varma, D.; Barnhart, L. E. *J. Neurobiol.* **2004**, *58*, 189.
(102) Sakato, M.; King, S. M. *J. Struct. Biol.* **2004**, *146*, 58.
(103) Iyer, L. M.; Leipe, D. D.; Koonin, E. V.; Aravind, L. *J. Struct. Biol.* **2004**, *146*, 11.
(104) Burgess, S. A.; Walker, M. L.; Sakakibara, H.; Knight, P. J.; Oiwa, K. *Nature* **2003**, *421*, 715.
(105) Burgess, S. A.; Knight, P. J. *Curr. Opin. Struct. Biol.* **2004**, *14*, 138.
(106) Berg, H. C. *Annu. Rev. Biochem.* **2003**, *72*, 19.
(107) Tang, H.; Bruan, T. F.; Blair, D. F. *J. Mol. Biol.* **1996**, *261*, 209.
(108) Yamaguchi, S.; Fujita, H.; Ishihara, A.; Aizawa, S.-I.; Macnab, R. M. *J. Bacteriol.* **1986**, *166*, 187.
(109) Blair, D. F.; Berg, H. C. *Science* **1988**, *242*, 1678.
(110) Young, H. S.; Dang, H.; Lai, Y.; DeRosier, D. J.; Khan, S. *Biophys. J.* **2003**, *84*, 571.

(111) Thomas, D. R.; Morgan, D. G.; DeRosier, D. J. *Proc. Natl. Acad. Sci. U.S.A.* **1999**, *96*, 10134.
(112) Suzuki, H.; Yonekura, K.; Namba, K. *J. Mol. Biol.* **2004**, *337*, 105.
(113) Khan, S.; Dapice, M.; Reese, T. S. *J. Mol. Biol.* **1988**, *202*, 575.
(114) Kojima, S.; Blair, D. F. *Biochemistry* **2001**, *40*, 13041.
(115) Blair, D. F. *FEBS Lett.* **2003**, *545*, 86.
(116) Lloyd, S. A.; Whitby, F. G.; Blair, D. F.; Hill, C. P. *Nature* **1999**, *400*, 472.
(117) Yonekura, K.; Maki-Yonekura, S.; Namba, K. *Nature* **2003**, *424*, 643.
(118) Ryu, W. S.; Berry, R. M.; Berg, H. C. *Nature* **2000**, *403*, 444.
(119) Darnton, N.; Turner, L.; Breuer, K.; Berg, H. C. *Biophys. J.* **2003**, *86*, 1863.
(120) Stock, D.; Leslie, A. G. W.; Walker, J. E. *Science* **1999**, *286*, 1700.
(121) Menz, R. I.; Walker, J. E.; Leslie, A. G. W. *Cell* **2001**, *106*, 331.
(122) Boyer, P. D. *Biochim. Biophys. Acta* **1993**, *1140*, 215.
(123) Abrahams, J. P.; Leslie, A. G. W.; Lutter, R.; Walker, J. E. *Nature* **1994**, *370*, 621.
(124) Noji, H.; Yasuda, R.; Yoshida, M.; Kinosita, K., Jr. *Nature* **1997**, *386*, 299.
(125) Nishizaka, T.; Oiwa, K.; Noji, H.; Kimura, S.; Muneyuki, E.; Yoshida, M.; Kinosita, K. *Nat. Struct. Mol. Biol.* **2004**, *11*, 142.
(126) Jiang, W.; Hermolin, J.; Fillingame, R. H. *Proc. Natl. Acad. Sci. U.S.A.* **2001**, *98*, 4966.
(127) Yasuda, R.; Noji, H.; Kinoshita, K., Jr.; Yoshida, M. *Cell* **1998**, *93*, 1117.
(128) Ishijima, A.; Doi, T.; Sakurada, K.; Yanagida, T. *Nature* **1991**, *352*, 301.
(129) Spudich, J. A. *Nature* **1994**, *372*, 515.
(130) Morel, J.-E.; D'Hahan, N. *Biochim. Biophys. Acta* **2000**, *1474*, 128.
(131) Svoboda, K.; Block, S. M. *Cell* **1994**, *77*, 773.
(132) Hunt, A. J.; Gittes, F.; Howard, J. *Biophys. J.* **1994**, *67*, 766.
(133) Soong, R. K.; Bachand, G. D.; Neves, H. P.; Olkhovets, A. G.; Montemagno, C. D. *Science* **2000**, *290*, 1555.
(134) Bachand, G. D.; Soong, R. K.; Neves, H. P.; Olkhovets, A.; Craighead, H. G.; Montemagno, C. D. *Nano Lett.* **2001**, *1*, 42.
(135) Schmidt, J. J.; Jiang, X.; Montemagno, C. D. *Nano Lett.* **2002**, *2*, 1229.
(136) Liu, H.; Schmidt, J. J.; Bachand, G. D.; Rizk, S. S.; Looger, L. L.; Hellinga, H. W.; Montemagno, C. D. *Nat. Mater.* **2002**, *1*, 173.
(137) Kaim, G.; Dimroth, P. *EMBO J.* **1998**, *17*, 5887.
(138) Bald, D.; Noji, H.; Yoshida, M.; Hirono-Hara, Y.; Hisabori, T. *J. Biol. Chem.* **2001**, *276*, 39505.
(139) Itoh, H.; Takahashi, A.; Adachi, K.; Noji, H.; Yasuda, R.; Yoshida, M.; Kinosita, K. *Nature* **2004**, *427*, 465.
(140) Braig, K.; Otwinowski, Z.; Hegde, R.; Boisvert, D. C.; Joachimiak, A.; Horwich, A. L.; Sigler, P. B. *Nature* **1994**, *371*, 578.
(141) Ditzel, L.; Lowe, J.; Stock, D.; Stetter, K.-O.; Huber, H.; Huber, R.; Steinbacher, S. *Cell* **1998**, *93*, 125.
(142) Wang, J.; Boisvert, D. C. *J. Mol. Biol.* **2003**, *327*, 843.
(143) Shimamura, T.; Koike-Takeshita, A.; Yokoyama, K.; Yoshida, M.; Taguchi, H.; Iwata, S. *Acta Crystallogr., Sect. D* **2003**, *D59*, 1632.
(144) Shomura, Y.; Yoshida, T.; Iizuka, R.; Maruyama, T.; Yohda, M.; Miki, K. *J. Mol. Biol.* **2004**, *335*, 1265.
(145) Chen, L.; Sigler, P. B. *Cell* **1999**, *99*, 757.
(146) Wang, J.; Chen, L. *J. Mol. Biol.* **2003**, *334*, 489.
(147) Xu, Z.; Horwich, A. L.; Sigler, P. B. *Nature* **1997**, *388*, 741.
(148) Ranson, N. A.; Farr, G. W.; Roseman, A. M.; Gowen, B.; Fenton, W. A.; Horwich, A. L.; Saibil, H. R. *Cell* **2001**, *107*, 869.
(149) Chaudhry, C.; Farr, G. W.; Todd, M. J.; Rye, H. S.; Brunger, A. T.; Adams, P. D.; Horwich, A. L.; Sigler, P. B. *EMBO J.* **2003**, *22*, 4877.
(150) Georgopoulos, C. P.; Hohn, B. *Proc. Natl. Acad. Sci. U.S.A.* **1978**, *75*, 131.
(151) Hunt, J. F.; Weaver, A. J.; Landry, S. J.; Gierasch, L.; Deisenhofer, J. *Nature* **1996**, *379*, 37.
(152) Grantcharova, V.; Alm, E. J.; Baker, D.; Horwich, A. L. *Curr. Opin. Struct. Biol.* **2001**, *11*, 70.
(153) Gierasch, L. M. *Mol. Cell* **2002**, *9*, 3.
(154) Taguchi, H.; Ueno, T.; Tadakuma, H.; Yoshida, M.; Funatsu, T. *Nat. Biotechnol.* **2001**, *19*, 861.
(155) Ueno, T.; Taguchi, H.; Tadakuma, H.; Yoshida, M.; Funatsu, T. *Mol. Cell* **2004**, *14*, 423.
(156) Trent, J. D.; Nimmesgern, E.; Wall, J. S.; Hartl, F. U.; Horwich, A. L. *Nature* **1991**, *354*, 490.
(157) McMillan, R. A.; Paavola, C. D.; Howard, J.; Chan, S. L.; Zaluzec, N. J.; Trent, J. D. *Nat. Mater.* **2002**, *1*, 247.
(158) Koeck, P. J. B.; Kagawa, H. K.; Ellis, M. J.; Hebert, H.; Trent, J. D. *Biochim. Biophys. Acta* **1998**, *1429*, 40.
(159) Ishii, D.; Kinbara, K.; Ishida, Y.; Ishii, N.; Okochi, M.; Yohda, M.; Aida, T. *Nature* **2003**, *423*, 628.
(160) Taguchi, H.; Konishi, J.; Ishii, N.; Yoshida, M. *J. Biol. Chem.* **1991**, *266*, 22411.

(161) Yurke, B.; Turberfield, A. J.; Mills, A. P., Jr.; Simmel, F. C.; Neumann, J. L. *Nature* **2000**, *406*, 605.
(162) Simmel, F. C.; Yurke, B. *Phys. Rev. E* **2001**, *63*, 041913.
(163) Feng, L.; Park, S. H.; Reif, J. H.; Yan, H. *Angew. Chem., Int. Ed.* **2003**, *42*, 4342.
(164) Yan, H.; Zhang, X.; Shen, Z.; Seeman, N. C. *Nature* **2002**, *415*, 62.
(165) Li, J. J.; Tan, W. *Nano Lett.* **2002**, *2*, 315.
(166) Alberti, P.; Mergny, J.-L. *Proc. Natl. Acad. Sci. U.S.A.* **2003**, *100*, 1569.
(167) Liu, D.; Balasubramanian, S. *Angew. Chem., Int. Ed.* **2003**, *42*, 5734.
(168) Chen, Y.; Lee, S.-H.; Mao, C. *Angew. Chem., Int. Ed.* **2004**, *43*, 5335.
(169) Sherman, W. B.; Seeman, N. C. *Nano Lett.* **2004**, *4*, 1203.
(170) Shin, J.-K.; Pierce, N. A. *J. Am. Chem. Soc.* **2004**, *126*, 10834.
(171) Tian, Y.; Mao, C. *J. Am. Chem. Soc.* **2004**, *126*, 11410.
(172) Dittmer, W. U.; Reuter, A.; Simmel, F. C. *Angew. Chem., Int. Ed.* **2004**, *43*, 3550.
(173) Turberfield, A. J.; Mitchell, J. C.; Yurke, B.; Mills, A. P., Jr.; Blakey, M. I.; Simmel, F. C. *Phys. Rev. Lett.* **2003**, *90*, 118102.
(174) Chen, Y.; Wang, M.; Mao, C. *Angew. Chem., Int. Ed.* **2004**, *43*, 3554.
(175) Chen, Y.; Mao, C. *J. Am. Chem. Soc.* **2004**, *126*, 8626.
(176) Feynman, R. P. *Eng. Sci.* **1960**, *23*, 22.
(177) Shinkai, S.; Ogawa, T.; Nakaji, T.; Kusano, Y.; Manabe, O. *Tetrahedron Lett.* **1979**, *20*, 4569.
(178) Shinkai, S.; Nakaji, T.; Nishida, Y.; Ogawa, T.; Manabe, O. *J. Am. Chem. Soc.* **1980**, *102*, 5860.
(179) Shinkai, S.; Nakaji, T.; Ogawa, T.; Shigematsu, K.; Manabe, O. *J. Am. Chem. Soc.* **1981**, *103*, 111.
(180) Shinkai, S.; Honda, Y.; Kusano, Y.; Manabe, O. *J. Chem. Soc., Chem. Commun.* **1982**, 848.
(181) Shinkai, S. *Pure Appl. Chem.* **1987**, *59*, 425.
(182) Shinkai, S. *Comprehensive Supramolecular Chemistry*; Gokel, G. W., Ed.; Elsevier Science Ltd.: Oxford, 1999; Vol. 1, pp 671–700.
(183) Feringa, B. L.; van Delden, R. A.; ter Wiel, M. K. J. *Pure Appl. Chem.* **2003**, *75*, 563.
(184) Mandl, C. P.; König, B. *Angew. Chem., Int. Ed.* **2004**, *43*, 1622.
(185) Koumura, N.; Zijistra, R. W. J.; van Delden, R. A.; Harada, N.; Feringa, B. L. *Nature* **1999**, *401*, 152.
(186) Koumura, N.; Geertsema, E. M.; Meetsma, A.; Feringa, B. L. *J. Am. Chem. Soc.* **2000**, *122*, 12005.
(187) Koumura, N.; Geertsema, E. M.; van Gelder, M. B.; Meetsma, A.; Feringa, B. L. *J. Am. Chem. Soc.* **2002**, *124*, 5037.
(188) van Delden, R. A.; Koumura, N.; Schoevaars, A.; Meetsma, A.; Feringa, B. L. *Org. Biomol. Chem.* **2003**, *1*, 33.
(189) Van Delden, R. A.; Koumura, N.; Harada, N.; Feringa, B. L. *Proc. Natl. Acad. Sci. U.S.A.* **2002**, *99*, 4945.
(190) Kelly, T. R.; De Silva, H.; Silva, R. A. *Nature* **1999**, *401*, 150.
(191) Kelly, T. R.; Silva, R. A.; De Silva, H.; Jasmin, S.; Zhao, Y. *J. Am. Chem. Soc.* **2000**, *122*, 6935.
(192) Kelly, T. R. *Acc. Chem. Res.* **2001**, *34*, 514.
(193) Leigh, D. A.; Wong, J. K. Y.; Dehez, F.; Zerbetto, F. *Nature* **2003**, *424*, 174.
(194) Bottari, G.; Dehez, F.; Leigh, D. A.; Nash, P. J.; Perez, E. M.; Wong, J. K. Y.; Zerbetto, F. *Angew. Chem., Int. Ed.* **2003**, *42*, 5886.
(195) Hannam, J. S.; Lacy, S. M.; Leigh, D. A.; Saiz, C. G.; Slawin, A. M. Z.; Stitchell, S. G. *Angew. Chem., Int. Ed.* **2004**, *43*, 3260.
(196) Hoki, K.; Yamaki, M.; Koseki, S.; Fujimura, Y. *J. Chem. Phys.* **2003**, *118*, 497.
(197) Hoki, K.; Yamaki, M.; Koseki, S.; Fujimura, Y. *J. Chem. Phys.* **2003**, *119*, 12393.
(198) Hoki, K.; Yamaki, M.; Fujimura, Y. *Angew. Chem., Int. Ed.* **2003**, *42*, 2976.
(199) Bissell, A.; Córdova, E.; Kaifer, A. E.; Stoddart, J. F. *Nature* **1994**, *369*, 133.
(200) Badjic, J. D.; Balzani, V.; Credi, A.; Silvi, S.; Stoddart, J. F. *Science* **2004**, *303*, 1845.
(201) Jimenez, M. C.; Dietrich-Buchecker, C.; Sauvage, J.-P. *Angew. Chem., Int. Ed.* **2000**, *39*, 3284.
(202) Jimenez-Molero, M. C.; Dietrich-Buchecker, C.; Sauvage, J.-P. *Chem.—Eur. J.* **2002**, *8*, 1456.
(203) Jimenez-Molero, M. C.; Dietrich-Buchecker, C.; Sauvage, J.-P. *Chem. Commun.* **2003**, 1613.
(204) Thordarson, P.; Bijsterveld, E. J. A.; Rowan, A. E.; Nolte, R. J. M. *Nature* **2003**, *424*, 915.
(205) Thordarson, P.; Nolte, R. J. M.; Rowan, A. E. *Aust. J. Chem.* **2004**, *57*, 323.
(206) Hollis, B. W. *Proc. Natl. Acad. Sci. U.S.A.* **1990**, *87*, 6009.
(207) Guengerich, F. P. *J. Biol. Chem.* **1991**, *266*, 10019.
(208) Muraoka, T.; Kinbara, K.; Kobayashi, Y.; Aida, T. *J. Am. Chem. Soc.* **2003**, *125*, 5612.
(209) Ichimura, K.; Oh, S.-K.; Nakagawa, M. *Science* **2000**, *288*, 1624.
(210) Sheiko, S. S.; Möller, M. *Chem. Rev.* **2001**, *101*, 4099.

(211) Xu, H.; Shirvanyants, D.; Beers, K.; Matyjaszewski, K.; Rubinstein, M.; Sheiko, S. S. *Phys. Rev. Lett.* **2004**, *93*, 206103.
(212) Yu, Y.; Nakano, M.; Ikeda, T. *Nature* **2003**, *425*, 145.
(213) Tabe, Y.; Yokoyama, H. *Nat. Mater.* **2003**, *2*, 806.
(214) Flood, A. H.; Ramirez, R. J. A.; Deng, W.-Q.; Muller, R. P.; Goddard, W. A., III; Stoddart, J. F. *Aust. J. Chem.* **2004**, *57*, 301.

(215) Collier, C. P.; Mattersteig, G.; Wong, E. W.; Luo, Y.; Beverly, K.; Sampaio, J.; Raymo, F. M.; Stoddart, J. F.; Heath, J. R. *Science* **2000**, *289*, 1172.
(216) Collier, C. P.; Jeppesen, J. O.; Luo, Y.; Perkins, J.; Wong, E. W.; Heath, J. R.; Stoddart, J. F. *J. Am. Chem. Soc.* **2001**, *123*, 12632.